Theoretical Determination of Absolute Electron-Impact Ionization Cross Sections of Molecules

ARTICLE *in* INTERNATIONAL JOURNAL OF MASS SPECTROMETRY · FEBRUARY 2000

Impact Factor: 1.97 · DOI: 10.1016/S1387-3806(99)00257-2

ELSEVIER

International Journal of Mass Spectrometry 197 (2000) 37–69

International Journal of Mass Spectrometry

Review

Theoretical determination of absolute electron-impact ionization cross sections of molecules

H. Deutsch[a], K. Becker[b], S. Matt[c], T.D. Märk[c,*]

[a]*Institut für Physik, Ernst Moritz Arndt Universität Greifswald, Domstr. 10a, D-17487 Greifswald, Germany*
[b]*Department of Physics, Stevens Institute of Technology, Hoboken, NJ 07030, USA*
[c]*Institut für Ionenphysik, Leopold Franzens Universität Innsbruck, Technikerstr. 25, A-6020 Innsbruck, Austria*

Received 6 September 1999; accepted 1 November 1999

Abstract

Much emphasis has been devoted recently to the experimental determination of absolute electron-impact ionization cross sections of molecules and radicals because of the importance of these cross sections in many applications (e.g. as input parameters to modeling codes for various purposes). Supporting theoretical calculations have been lagging behind to some extent. Because of the inherent complexity of such calculations, simplistic additivity rules and semiempirical methods have often been used in place of more rigorous calculation schemes, particularly in applications where a larger number of cross section data were needed with reasonable precision. Although these methods have often proved to be quite successful as descriptive tools (i.e. reproducing existing experimental ionization cross sections reasonably well), their ability to calculate cross sections for species for which no experimental data are available (predictive capabilities) tend to be limited or questionable. This topical review describes recent progress in the development of more rigorous approaches for the calculation of absolute electron-impact molecular ionization cross sections. The main emphasis will be on the application of the semiclassical Deutsch–Märk (DM) formalism, which was originally developed for the calculation of atomic ionization cross sections, to molecular targets, and on the binary–encounter–Bethe (BEB) method of Kim and Rudd. The latter is a simpler version of the more rigorous binary–encounter–dipole (BED) theory, which was also first developed for the calculation of atomic ionization cross sections, and based on the methods developed by Khare and co-workers. Extensive comparisons between available experimental cross sections and the predictions of these theoretical models will be made for 31 molecules and free radicals (H_2, N_2, O_2, S_2, C_2, C_3, O_3, H_2O, NH_3, CO_2, CH_4, CH_3, CH_2, CH, CF_4, CF_3, CF_2, CF, NF_3, NF_2, NF, SiF_3, SiF_2, SiF, $TiCl_4$, C_2H_2, C_2H_6, C_6H_6, SiF_6, C_2F_6, CH_3OH). (Int J Mass Spectrom 197 (2000) 37–69) © 2000 Elsevier Science B.V.

Keywords: Electron-impact ionization; Cross section calculations; Molecules

* Corresponding author. Also adjunct professor at Dept. Plasmaphysics, Univerzita Komenskeho, Mlynska dolina, SK-842 15 Bratislava 4, Slovak Republic. E-mail: Tilmann.Maerk@uibk.ac.at

PII S1387-3806(99)00257-2

1. Introduction

Electron interaction with matter leading to ionization is one of the most fundamental processes in collision physics. Cross sections for electron-impact ionization have been measured and calculated since the early days of collision physics [1] because of their basic importance to the kinetics and dynamics of collisions and because of their relevance in many practical applications. Considerable progress in the experimental determination of cross sections for atomic and molecular targets [2–6] has been achieved in the past decade. Electron-impact ionization cross sections of molecules are important quantities in a variety of applications as diverse as low-temperature processing plasmas, fusion edge plasmas, gas discharges, planetary, stellar, and cometary atmospheres, radiation chemistry, mass spectrometry, and chemical analysis [2]. Rigorous quantum mechanical calculations of ionization cross sections for molecular targets are beyond the capability of current quantum-mechanical electron collision theory for essentially all molecules [7–9]. The need to incorporate molecular ionization cross sections in modeling codes for various applications (e.g. in fusion edge plasmas [10] and in plasma processing [11]) has stimulated the use of simplistic additivity rules to estimate molecular ionization cross sections. Many variants of the additivity rule, a concept that was first introduced by Ötvos and Stevenson [12] can be found in literature [13,14]. They all rely on the concept that the molecular ionization cross section is derived by adding in some fashion the ionization cross sections of the atomic constituents of the molecule with or without accounting for molecular bonding and/or weighting factors for the atomic cross sections.

The most recent variant of the additivity rule is the so-called modified additivity rule (MAR) of Deutsch and co-workers [15,16] that includes appropriately chosen weighting factors to account for molecular bonding. Predictions of the MAR have been compared to available experimental cross section data for many molecules with sum formulas of the form AB_x [15] and A_xB_y, $A_xB_yC_z$, and $A_pB_sC_tD_u$ [16] and reasonable agreement was found in essentially all cases. In addition to these additivity approaches, there have been other conceptually simplistic (geometric) methods such as (1) the geometric approach of Kistemaker and co-workers [17] that considers different electron–molecule approach geometries and calculates the ionization cross section by averaging over all possible orientations, and (2) a theory based on the calculation of the maximum in the electron-impact ionization cross section as a function of the electron–molecule approach geometry and subsequent averaging over the different orientations [18–20].

In contrast there now exist more rigorous methods [21–28] including (1) the Deutsch–Märk (DM) formalism that combines a Gryzinski-type energy dependence of the cross section with quantum mechanically calculated molecular structure information based on an additivity concept [21–23], (2) the method of Khare and co-workers [24,25], that combines two cross section expressions (the Mott and Bethe cross section) describing ionizing collisions that occur at large impact parameters and at small impact parameters, respectively, and (3) the binary–encounter–Bethe (BEB) theory of Kim, Rudd, and co-workers [26–28], which in addition to combining two cross section expressions (the binary encounter and Bethe cross section), also introduces an additivity concept with quantum mechanically calculated molecular quantities.

This article presents a topical review of the status of calculations of absolute electron-impact ionization cross sections for molecules and radicals with special emphasis on the DM formalism and the BEB formalism, which are the most widely used calculation schemes among those methods that may be labeled “more rigorous” theoretical approaches. Both methods incorporate quantum mechanically calculated molecular structure information—a fact that sets them apart from the more simplistic additivity rules and the purely geometric methods. It is noteworthy to point out in this context that both the DM formalism and the BEB formalism also make use of an additivity *concept* in the sense that the ionization cross section of a molecule is obtained by summing up the contributions arising from the ejection of an electron from the different molecular orbitals [29]. This has sometimes

led people to erroneously refer to the DM and BEB calculations as variants of the additivity *rule*. We would like to make a clear distinction between simplistic additivity rules (like the ones mentioned above [12–20]) and more rigorous methods like the DM formalism and the BEB formalism that include quantum mechanically calculated molecular structure information, even though these approaches also incorporate an additivity concept in some fashion. The method of Khare and co-workers can also be classified as a more rigorous theoretical approach, but it has only been applied to a limited number of target molecules. Extensive comparisons will be made between calculated ionization cross sections using the DM formalism and the BEB formalism and experimentally determined cross sections for more than 31 molecules and radicals. We included ionization cross section predictions obtained by Khare and co-workers for those molecules for which such calculations were available.

2. Theoretical background

In this section we describe briefly the concepts and the historical development of the DM formalism, the method of Khare and co-workers, and the BEB formalism of Kim and Rudd. We will begin with a brief discussion of the formalisms developed by Khare and co-workers and by Kim and Rudd, that in some sense have a common origin. We will subsequently review the development of the DM formalism that was developed from a different point of view.

2.1. Formalisms combining cross section expressions

Inelastic collisions between electrons and atoms may be divided into two broad categories: soft (or distant) collisions that occur at large impact parameters and hard (or close) collisions that occur at small impact parameters. The Mott cross section formalism [30], which is a generalized Rutherford cross section [31] taking into account electron exchange effects, describes the collision of two free electrons, thus accounting well for hard collisions. Conversely, using the first Born approximation [32], Bethe [33] derived a cross section formula for the dipole interaction involving fast incident electrons and thus accounting well for soft collisions. Attempts have been made by various authors (see Miller et al. [34] and references therein) to combine the dipole interaction with free electron collisions in order to arrive at a "correct" ionization cross section formula that is essentially free of adjustable or fit parameters. All early attempts had only limited success because they failed to find the "correct" mixing ratio between the soft and hard collision terms. Two groups recently revisited this problem again with more success. The group of S.P. Khare and co-workers at the Meerut University in India and a collaboration between M.E. Rudd at the University of Nebraska and Y.-K. Kim at NIST. As will be shown in the following sections where we will describe in detail these developments, both approaches involve approximations in deriving the corresponding expressions (cross sections) and, in addition, both approaches require certain input parameters that are not always readily available, e.g. (differential) dipole oscillator strengths.

2.1.1. The formalism of Khare and co-workers

The first successful attempt to calculate total (counting) [29] ionization cross sections for molecules using a combination of theories describing the two different types of collisions mentioned above was made by Khare and co-workers in 1976 [24,35] (see also the earlier work of Khare and co-workers on total ionization cross sections for the rare gases [36]). This work was based on earlier work to (1) calculate [37] energy-loss cross sections $d\sigma(E, w)/dw$, where E is the energy of the incident electron and w is the energy loss suffered by the incident electron in the ionizing collision and (2) to calculate [38,39] the single differential ionization cross section $d\sigma(E, \varepsilon)/d\varepsilon$ for the production of a secondary electron of energy ε, with $w = \varepsilon + E_i$, where E_i refers to the ionization energy. The total ionization cross section $\sigma(E)$ is then obtained by integration over all possible values of ε

from 0 to $(E - E_i)/2$. Moreover, Khare and coworkers [25,40–44] recently extended their formalism to the calculation of partial ionization cross sections of molecules (that is, the cross section for the production of a specific parent or fragment ion, see [2]).

As summarized by these authors [24,40], according to Inokuti [32] the single differential ionization cross section $d\sigma(E, \varepsilon)/d\varepsilon$ is given in the first Born approximation by

$$d\sigma(E, \varepsilon)/d\varepsilon = (4\pi a_0^2 R^2/Ew) \times \int (\delta f(w, K^2a_0^2)/\delta w) d[\ln(Ka_0)^2] \quad (1)$$

where a_0 denotes the Bohr radius, R the Rydberg energy (ionization energy E_i of the hydrogen atom), $\delta f(w, K^2a_0^2)/\delta w$ is the density of the generalized oscillator strength per unit energy range, and Ka_0 is the change in the momentum vector of the incident electron due to scattering. The generalized oscillator strength may be given in a complete fashion by plotting $\delta f/\delta w$ versus $\ln[(Ka_0)^2]$ and w/R (Bethe surface). Depending on the nature of the energy transfer—"hard" collisions are associated with a large energy transfer and "soft" (glancing) collisions with a small energy transfer—ionizing collisions can be divided into two regimes on this Bethe surface. Eq. (1) is reduced to the Bethe term for soft collisions where the collisions take place primarily through the dipole interaction between the incident electron and the target electron (see Miller and Platzmann [45])

$$d\sigma(E, \varepsilon)/d\varepsilon|_B = (4\pi a_0^2 R^2/Ew) \times (\delta f(w, 0)/\delta w) \ln[CE] \quad (2)$$

Here $\delta f(w, 0)/\delta w$ is the differential optical oscillator strength for the ionization of the molecule by a photon of energy w and $C(w)$ is the collisional parameter as defined in [45]. One can see that the Bethe cross section exhibits the characteristic asymptotic energy dependence $\ln E/E$ that arises from the dipole interaction. In the case of hard collisions, the differential cross section is given by the Mott term that describes the collision of two free electrons

$$d\sigma(E, \varepsilon)/d\varepsilon|_M = 4\pi a_0^2 R^2 s \times (1/\varepsilon^2 - 1/(E - \varepsilon)\varepsilon + 1/(E - \varepsilon)^2)/E \quad (3)$$

where s is the number of electrons that participate in these hard collisions. The first term in the bracket corresponds to the direct collision term (as used in the Rutherford cross section), the second term represents the interference between the direct and exchange term, and the third term accounts for the exchange effects. As expected, the Mott cross section is symmetric in terms of the kinetic energies of the outgoing electrons, i.e. in terms of ε and $(E - \varepsilon)$ for the "secondary" (or ejected) electron and the "scattered" electron, respectively.

Both Eqs. (2) and (3) are valid in the limit of high incident electron energies. To extend the range of their validity to low incident energies, Khare and co-workers added the two cross sections after multiplying each cross section by an arbitrary factor, f_1 and f_2, which were chosen by the authors [24] to obtain satisfactory agreement with experimental data

$$d\sigma(E, \varepsilon)/d\varepsilon = f_1 d\sigma(E, \varepsilon)/d\varepsilon|_B + f_2 d\sigma(E, \varepsilon)/d\varepsilon|_M \quad (4)$$

with

$$f_1(E, \varepsilon) = [1/(1 - E_i/E)] \times (1 - \varepsilon(E - E_i) \ln[1 - C(E - E_i)]/\ln[CE] \quad (5)$$

and

$$f_2(E, \varepsilon) = [\varepsilon^3/(\varepsilon^3 + \varepsilon_0^3)](1 - E_i/E) \quad (6)$$

thereby extrapolating the Bethe and Mott cross sections to low incident electron energies and controlling the mixing of soft and hard collisions. Here ε_0 denotes a "mixing parameter" (see below for a definition of ε_0). Thus, $f_1 d\sigma(E, \varepsilon)/d\varepsilon|_B$ dominates the single differential cross section for small values of ε and $f_2 d\sigma(E, \varepsilon)/d\varepsilon|_M$ dominates the single differential cross section for large values of ε.

As we will see later, the total cross sections $\sigma(E)$

obtained by Khare and co-workers using this formalism after proper integration $\sigma(E) = \int (d\sigma(E, \varepsilon)/d\varepsilon)d\varepsilon$ was found to agree reasonably well with experimental results in many cases. It should be mentioned, however, that in order to apply the method of Khare and co-workers, which involves an "educated guess" of the ratio of the Mott cross section to the Bethe cross section, several prerequisites are necessary that preclude the application of this formalism to a wider range of target molecules. In addition to experimental or theoretical values for the ionization energy E_i of the target molecule, one needs for each molecule information on the mixing parameter ε_0, on the dipole oscillator strength $\delta f(w, 0)/\delta w$, and on the collision parameter $C(w)$. The value of the mixing parameter has been chosen [24] in such a way as to obtain the best agreement with experimental differential ionization cross section data $d\sigma(E, \varepsilon)/d\varepsilon$ at $E =$ 500 eV (as, for instance, reported in [46]). Information about the dipole oscillator strength (problems that may arise in the integration necessary for the determination of the total cross sections [24] are discussed in [47]) and about the collision parameter are obtained from experimental photon ionization and electron ionization data, respectively. In the case of $C(w)$, Khare and co-workers assumed C to be independent of w and to be equal to the experimentally determined high energy limit (as, for instance, deduced from the counting cross section data of [48]).

By extending the approach of Khare and co-workers, Saksena et al. [49] demonstrated recently that based on an approach by Mayol and Salvat [50], no a priori knowledge of the mixing parameter ε_0 and the collision parameter C is necessary and thus, calculations can be carried out for all molecules for which total photoionization cross section data are available. In Sec. 3 we will compare (when available) experimental data with both the results of the formalism of Khare and co-workers [24,25] and the results of the calculations of Saksena et al. [49].

Moreover, it is interesting to note that Khare and co-workers [51] recently combined the features of the approach of Saksena et al. [49] and that of Kim and Rudd [26] (see below). According to these authors [51] they arrived at expressions for the total ionization cross section in the BED and BEB formulations (see below) that are close to the results from Kim and Rudd [26]. See the results given here for the case of CH_4 in Sec. 3 (see also Figs. 1 and 2 in [51]).

2.1.2. The formalism of Kim and Rudd

In 1994, Kim and Rudd [26] extended the previous approach in several ways. First, they used the binary encounter approximation (BEA) (see Vriens [52] for its symmetric form), where a velocity or momentum distribution is ascribed to the target particle to replace the Mott cross section. Such a momentum distribution is frequently derived from the wave function of the target particle. Thus, the symmetric form of the BEA cross section differs from the Mott cross section by an extra term incorporating the average kinetic energy KE of the target electron. Kim and Rudd then combined this modified form of the Mott cross section and the Bethe cross section by requiring the ionization cross section and the corresponding stopping cross section to satisfy the high energy asymptotic behavior of the Bethe theory. After some further approximations that are described in detail in [26] the single differential ionization cross section for a particular subshell is given in what Kim and Rudd refer to as the BED model by

$$\begin{aligned} d\sigma(E, \varepsilon)/d\varepsilon = {} & 4\pi a_0^2 (R/E_j)^2 \xi/E_j (t + u + 1) \\ & \times \{([(N_i/\xi) - 2]/(t + 1))[(1/(w \\ & + 1) + 1/(t - w)] + [2 - (N_i/\xi)] \\ & \cdot [(1/(w + 1)^2 + 1/(t - w)^2] \\ & + [\ln(t)/\xi(w + 1)][df(w)/dw]\} \end{aligned} \tag{7}$$

where E_j is the binding energy of the ejected electron, ξ is the number of bound electrons in that particular subshell j, $t = E/E_j$, $w = \varepsilon/E_j$, $u = KE/E_j$, $N_i = \int [df(w)/dw]dw$, and $[df(w)/dw]$ denotes the differential oscillator strength. The total ionization cross section, which is obtained by integrating the differen-

tial cross section, is then given by the simple expression

$$\sigma(E) = 4\pi a_0^2 (R/E_j)^2 \xi/(t + u + 1)\{D(t)\ln(t) + [2 - (N_i/\xi)][(t-1)/t - \ln(t)/(t+1)]\} \quad (8)$$

with

$$D(t) = \xi^{-1} \int [1/(1+w)][df(w)/dw]\, dw \quad (9)$$

integrated from 0 to $(t - 1)$ according to [51] [and not to $(t - 1)/2$ as given in the original reference].

The above given cross sections are for a specific subshell and the cross section σ for the entire target must be summed over all subshells that contribute to the ionization yield. It is clear that in addition to information on E_j and ξ, the differential oscillator strengths are needed for each subshell of the target. The average kinetic energy KE needed in the BED model is a theoretical quantity that can be obtained from quantum chemistry codes (and thus from an explicit knowledge of molecular wave functions). Average kinetic energies for subshells of some atoms and molecules are listed in [53] (see also the various articles by Kim, Rudd, and co-workers [26–28,54,55]). Differential oscillator strengths for specific subshells are even harder to obtain; some of these are summarized in [56,57] and in articles by Kim, Rudd, and co-workers.

Because it is often difficult to obtain the above quantities for all subshells and, in particular, for the various subshells of molecules, Kim and Rudd devised a simpler version of the BED approach that is referred to as the BEB model [26,27]. As argued by Kim and Rudd, the quantity $df(w)/dw$ is not known for most molecules for the individual orbitals. In these cases, Kim and Rudd replaced $df(w)/dw$ by a simple analytical expression describing the ground state hydrogen case

$$df(w)/dw = b/(w+1)^2 \quad (10)$$

where b is a constant equal to N_i. With this simplification, the authors arrive at the BEB cross section $\sigma_Q(E)$ per molecular orbital

$$\sigma_Q(E) = 4\pi a_0^2 (R/E_j)^2 \xi/(t+u+1)\{[(Q\ln(t))/2] \times (1 - 1/t^2) + [2 - Q][(t-1)/t - \ln(t)/(t+1)]\} \quad (11)$$

in terms of the integrated dipole quantity Q

$$Q = (2E_j/\xi R) m_{\text{ion}}^2 \quad (12)$$

with

$$m_{\text{ion}}^2 = (R/E_j) \int [1/(1+w)](df(w)/dw)\, dw \quad (13)$$

integrated from 0 to ∞. This equation has been further simplified when Q (and thus m_{ion}^2 and df/dw) is unknown by simply assuming $Q = 1$ (which means $m_{\text{ion}}^{-2} = 2E_j/\xi R$ for individual orbitals). The corresponding ionization cross section is then called σ_{BEB}. Kim and Rudd, however, warn in their original article [26] that "the reliability of resulting cross sections may suffer in this case." In a later article, Kim, Rudd, and co-workers [54] come to the conclusion that "assuming $Q = 1$ . . . has been shown to be an excellent approximation for many molecules."

In Sec. 3 we will include both BED and BEB calculations for comparison with experimental data and the various results of Khare and co-workers for those molecules where these calculations are available.

2.2. The DM formalism

The formalism introduced by Deutsch and Märk [58] has a different origin from the previously discussed formalisms of Khare and co-workers and Kim and Rudd. The original concept of Deutsch and Märk [58], which was developed for the calculation of atomic ionization cross sections, has been modified and extended several times. We begin with a brief outline of the original DM approach and the subsequent modifications that resulted in a very general formula now applicable to the single ionization of ground-state [58,59] and excited-state (metastable)

atoms [60,61], the removal of a specific single outershell [62] and innershell electron [63] of atoms as well as to the single ionization of molecules [21], radicals [22,23], small Ag, H_2, and CO_2 clusters, and C_{60} [64–66] and atomic ions [67,68] as well as to the multiple ionization of atoms [69–72]. In all cases, only direct ionization processes are considered in the original DM formalism (i.e. the prompt removal of a single electron from the electron shell by the incoming electron—therefore it is not possible to distinguish between single and multiple ionization when innershell electron ejection occurs). Two-step ionization mechanisms such as autoionization after innershell excitation cannot be described by the DM formalism (nor by any of the other methods described above).

Thomson [73] was the first to derive a formula for the electron-impact ionization cross section of an atom using a classical binary encounter approximation. This classical treatment was modified by several authors using different initial conditions. Gryzinski [74] introduced the concept of a continuous velocity distribution for atomic electrons, which resulted in an expression for the ionization cross section σ of the form

$$\sigma = \sum_{n,l} 4\pi(a_0)^2 \xi_n (R/E_{nl})^2 f(U) \tag{14}$$

with

$$f(U) = d(1/U)[(U-1)/(U+1)]^a \times \{b + c[1 - (1/2U)] \ln [2.7 + (U-1)^{0.5}]\} \tag{15}$$

and

$$a = 3/2,\ b = 1,\ c = 2/3, \text{ and } d = 1 \tag{16}$$

Here ξ_n is the number of electrons in the nth atomic subshell, and E_{nl} refers to the ionization energy in the nth subshell, and U is the reduced energy given by $U = E/E_{nl}$ where E is the energy of the incident electron. However, even this improved cross section formula fails for some rather simple atoms such as neon, nitrogen, and fluorine [58,75].

Deutsch and Märk [58] suggested replacing the Bohr radius a_0 in Eq. (14) with the radius r_{nl} of the corresponding electronic subshell (labeled by the quantum numbers n and l) on the basis of a comparison between the classical binary encounter formula and the quantum mechanical Born–Bethe formula [33]. Support for this substitution comes from (1) the application of the Bethe formalism to the ionization cross section of an atomic electron with quantum numbers (n, l) giving results approximately proportional to the mean square radius $\langle r^2 \rangle$ of the (n, l) subshell [76,77] and (2) from the experimental observation of the existence of a correlation between the maximum of the atomic ionization cross section and the sum of the mean square radii of all outer electrons [78]. Subsequently, Margreiter et al. [59,60] successfully applied the following semiclassical formula to the calculation of the absolute electron-impact ionization cross section σ of a large number of ground-state and excited-state atoms

$$\sigma = \sum_{n,l} g_{nl} \pi (r_{nl})^2 \xi_{nl} f(U) \tag{17}$$

where r_{nl}^2 is the mean square radius of the (n, l) subshell and g_{nl} are weighting factors that were originally introduced by Bethe [33]. Bethe [33] calculated these "Ionisierungsfaktoren" as a function of the quantum numbers n and l using hydrogenic wave functions. By contrast, the generalized weighting factors g_{nl} introduced by Margreiter et al. [59,60] were obtained from a fitting procedure using reliable experimental ionization cross section data for the rare gases and uranium [2]. In a first approximation, these weighting factors were taken to be three for s electrons and 0.5 for all other electrons [58]. Subsequently, a more detailed analysis revealed that the g_{nl} are not constants, but depend on the quantum numbers n and l, and on the ionization energy E_{nl} in such a way that the product $g_{nl} \times E_{nl}$ (referred to as the "reduced weighting factor") is independent of the nuclear charge Z for completely filled subshells [60]. Furthermore, the results of recent calculations of K shell ionization cross sections [removal of a (1s) electron] for 11 atoms [79] using the DM formalism suggested a revision of the low-energy dependence of the calculated DM ionization cross sections for atoms whose ionization cross section at low energies is dominated by the removal of an s electron (e.g. H and

Table 1
Values of the reduced weighting factors $g_{nl} \times E_{nl}$ for electrons in the various (n, l) atomic subshells

Valence electron (n, l), number in subshell	Reduced weighting factors $g_{nl} \times E_{nl}$
(1*s*), 1	38.20
(1*s*), 2	70.00
(2*s*), 1	12.00
(2*s*), 2	20.00
(2*p*), 1	32.50
(2*p*), 2–6	30.00
(3*s*), 1	9.80
(3*s*), 2	14.00
(3*p*), 1	31.50
(3*p*), 2–4	25.00
(3*p*), 5–6	22.00
(3*d*), 1–10	13.60
(4*s*), 1	7.40
(4*s*), 2	10.00
(4*p*), 1	31.00
(4*p*), 2–4	22.40
(4*p*), 5	18.50
(4*p*), 6	17.50
(4*d*), all electrons	11.20
(4*f*), all electrons	20.00
(5*s*), 1	6.35
(5*s*), 2	7.5
(5*p*), 1	30.50
(5*p*), 2–4	20.00
(5*p*), 5	16.00
(5*p*), 6	13.00
(5*d*), all electrons	8.85
(5*f*), all electrons	1.00
(6*s*), 1	5.40
(6*s*), 2	6.00
(6*p*), 1	30.00
(6*p*), 2–4	18.00
(6*p*), 5	14.50
(6*p*), 6	7.50
(6*d*), all electrons	6.50

the alkalis Li, Na, K, and Cs). Along this line a detailed comparison between calculated alkali atom ionization cross sections using the DM formalism and experimental data [80] further substantiated this slight revision in the weighting factors g_{ns} for the *s* electrons. Table 1 summarizes the final set of the reduced weighting factors $g_{nl} \times E_{nl}$ for electrons in the various (n, l) subshells. Moreover, the parameters *a*, *b*, *c*, and *d* were also found to have different values for *s*, *p*, *d*, and *f* electrons as one might expect on the basis of the different angular shapes of atomic *s*, *p*, *d*, and *f* orbitals. In the course of revising the alkali ionization cross sections [80], it was also found necessary to revise the values of the parameters *a*, *b*, *c*, and *d* for the *s* electrons slightly as compared to the values reported earlier [59]. Table 2 summarizes the values for the parameters *a*, *b*, *c*, and *d* for *s*, *p*, *d*, and *f* electrons.

Table 2
Parameters *a*, *b*, *c*, and *d* for the energy dependent function in Eq. (17) for *s*, *p*, *d*, and *f* electrons

s electrons	*p* electrons	*d* electrons	*f* electrons
$a = 1.06$	$a = 2$	$a = 3/2$	$a = 3/2$
$b = 0.23$	$b = 1$	$b = 3$	$b = 1$
$c = 1$	$c = 1$	$c = 2/3$	$c = 2/3$
$d = 1.1$	$d = 1$	$d = 1$	$d = 1$

The straightforward extension of the DM formula of Eq. (17) to molecular targets [21] results in an equation of the form

$$\sigma = \sum_j g_j \pi (r_j)^2 \xi_j f^*(U) \tag{18}$$

where the summation is now carried out over the molecular orbitals labeled "*j*." Several problems with the application of this formula to molecules are immediately obvious: (1) a new set of weighting factors g_j would have to be determined either empirically or by ab initio calculations which is impractical, if not impossible, because each molecular symmetry group would probably require a separate set of weighting factors, (2) it is not clear how one could determine (or even define) a mean square radius $(r_j)^2$ for different molecular orbitals, and (3) a new energy-dependent function $f^*(U)$ would have to be determined, perhaps depending on the character of the molecular electrons (σ, π, δ, etc.), because the exact form of the previously introduced function $f(U)$ depends on the orbital angular momentum quantum number of the atomic electrons.

It was found much more advantageous [21–23] to reduce the case of a molecular ionization cross section calculation using the DM formalism to the previously derived atomic ionization cross section formula of Eq.

Table 3
Mulliken population of the water molecule (H_2O) from [85]

Molecular level j and occupancy	E_j (eV)	Atomic subshell (nl), ξ_{nl} value
$(1b_1)$, 2 electrons	12.6	O(2p),2.00
$(3a_1)$, 2 electrons	14.7	O(2p),1.46
		O(2s),0.20
		H(1s),0.34
$(1b_2)$, 2 electrons	18.5	O(2p),1.18
		H(1s),0.82
$(2a_1)$, 2 electrons	32.2	O(2p),1.50
		H(1s),0.50
$(1a_1)$, 2 electrons	539.7	O(1s),2.00

(17). This requires a Mulliken population analysis [81,82] (or an equivalent method) that expresses the molecular orbitals in terms of the atomic orbitals of the constituent atoms. As a result, each term in the above sum over "j" in Eq. (18) is expressed in terms of the appropriate atomic weighting factors $g^j_{A,(nl)}$, effective occupation numbers $\xi^j_{A,(nl)}$, mean square atomic radii $r^j_{A,(nl)}$, and functions $f^j_{A,(nl)}(U)$ where "A" labels the various constituent atoms of the molecule under study. A Mulliken population analysis can be obtained routinely for most molecules and radicals for which molecular structure information is available (see e.g. [83]) using standard quantum chemistry codes, many of which are available in the public domain. One of the most widely used and most versatile quantum chemistry codes in the public domain is the "NWChem" code [84]. It is noteworthy to point out that a Mulliken population analysis does not result in a unique representation of the molecular orbitals in terms of the atomic orbitals of the constituent atoms. Any Mulliken representation requires the optimization of a macroscopic parameter of the molecule (e.g. molecular geometry, dipole moment, polarizability, ionization energy, etc.) and depends on the atomic wave functions used to represent the constituent atoms. The "NWChem" code, for instance, gives the user the option to choose from more than 50 different atomic basis sets for the most common atoms [84]. A Mulliken representation of the water (H_2O) molecule taken from [85] is shown in Table 3. Not included in Table 3 are the mean square radii of the atomic subshells that can be taken from the compilation of Descleaux [86], and the weighting factors g_{nl} that can be obtained from the ionization energies E_j listed in Table 3 in conjunction with the reduced weighting factors listed in Table 1. We note that this particular Mulliken representation reproduces the well-known lowest ionization energy of the H_2O molecule of 12.61 eV [87] very well.

Table 4
Mulliken representations of the three outermost shells of the H_2O molecule using different atomic basis sets

Atomic basis set[a]	Molecular level j and occupancy	E_j (eV)	Atomic subshell (nl), ξ_{nl} value
[85]	$(1b_1)$, 2 electrons	12.6	O(2p), 2.00
[85]	$(3a_1)$, 2 electrons	14.7	O(2p), 1.46
			O(2s), 0.20
			H(1s), 0.34
[85]	$(1b_2)$, 2 electrons	18.5	O(2p), 1.18
			H(1s), 0.82
6-311G**	$(1b_1)$, 2 electrons	13.3	O(2p), 2.00
6-311G**	$(3a_1)$, 2 electrons	15.2	O(2p), 1.36
			O(2s), 0.64
			H(1s), 0.00
6-311G**	$(1b_2)$, 2 electrons	19.0	O(2p), 1.41
			H(1s), 0.59
STO-6G	$(1b_1)$, 2 electrons	10.9	O(2p), 2.00
STO-6G	$(3a_1)$, 2 electrons	12.7	O(2p), 1.18
			O(2s), 0.52
			H(1s), 0.30
STO-6G	$(1b_2)$, 2 electrons	16.7	O(2p), 0.97
			H(1s), 1.03
cc-pVTZ	$(1b_1)$, 2 electrons	13.5	O(2p), 2.00
cc-pVTZ	$(3a_1)$, 2 electrons	15.4	O(2p), 1.48
			O(2s), 0.52
			H(1s), 0.00
cc-pVTZ	$(1b_2)$, 2 electrons	18.8	O(2p), 1.52
			H(1s), 0.48

[a]The names of the basis sets are the same as those in the ECCE (extensible computational chemistry environment) basis set database as developed and distributed by the Molecular Science Computing Facility, Environmental and Molecular Science Laboratory at the Pacific Northwest National Laboratory, P.O. Box 999, Richland, WA 99352.

It is important in the context of the application of the DM formalism to molecular targets to realize the sensitivity of the calculations to the Mulliken representation of the molecular orbitals in terms of atomic orbitals of the constituent atoms. Table 4 summarizes

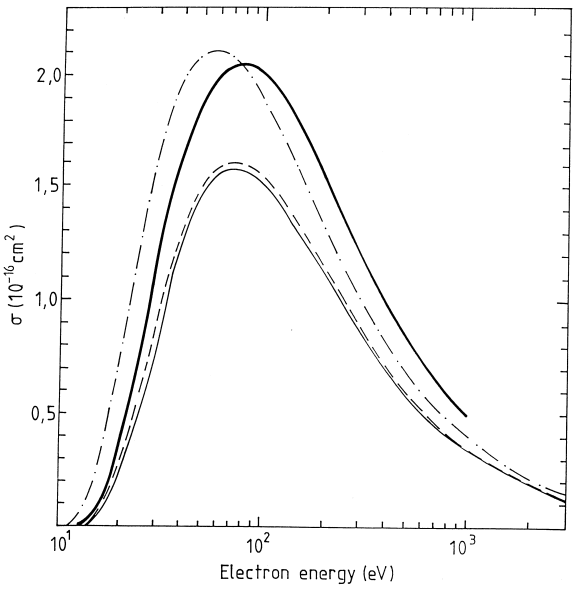

Fig. 1. Calculated H_2O ionization cross sections using the DM formalism with four different atomic basis sets employed in the Mulliken population analysis (see Table 4 for details). The four calculated curves correspond to the following basis sets: thick solid line ([85]), thin solid line (6-311G**), dash-dot line (STO-6G), and dashed line (cc-pVTZ).

the result of four different Mulliken representations of the three outermost molecular shells of the H_2O molecule (whose contributions essentially determine the H_2O ionization cross section) using four different atomic basis sets. It is apparent that there are significant differences in the ionization energies of the three shells and in their atomic representations depending on the particular choice for the atomic basis set. Although all four representations agree that the outermost H_2O orbital is purely of O($2p$) character, there are already significant differences in the representation of the second orbital, with two of the four basis sets ascribing pure O character, O($2p$), and O($2s$) to it, whereas the other two basis sets also show a H($1s$) contribution in the representation of this shell. In addition, there are significant differences in the ionization energies of the three orbitals. Fig. 1 shows the calculated H_2O DM ionization cross sections resulting from the four different Mulliken representations. As one can see, there are differences in the maximum cross section value of about 25% as well as a 15 eV difference in the energetic position of the maximum depending on the particular choice of the Mulliken representation.

3. Results and discussion

3.1. Selected hydrocarbon compounds [CH_x (x = 1–4), C_2H_6, C_2H_2, C_6H_6]

Hydrocarbon molecules are abundant constituents of planetary and cometary atmospheres and they also play an important role in combustion processes. More recently, hydrocarbons have also been used as feed gas constituents of low-temperature plasmas employed in the plasma-assisted deposition of diamond films and carbon films.

CH_4: Methane, CH_4, is one of the most abundant and important hydrocarbon compounds. The ionization of CH_4 has been studied by several experimental groups over a period of many years. Fig. 2 shows six experimental data sets of measured CH_4 ionization cross sections [88–93] in comparison with the present calculation, a calculation using the method of Khare and co-workers [24], a BEB calculation reported by Kim et al. [28], a BEB and BED calculation as reported by Khare et al. [51], and a calculation [51] using the method of Saksena et al. [49]. We note that there are other available experimental data in the literature, but these were either in very good agreement with those data sets shown in Fig. 2 (and omitted for reasons of clarity of presentation) or they were considered less reliable and/or obtained by experimental techniques that are now known to be susceptible to systematic uncertainties (see e.g. Basner et al. [6], Becker and Tarnovsky [11], Tarnovsky and Becker [94], and references therein to earlier work). The experimental data sets shown here are all in mutual agreement within their stated margins of error and they are all also in good agreement with the various calculated cross section curves. Overall, the CH_4 ionization cross section can thus be classified as

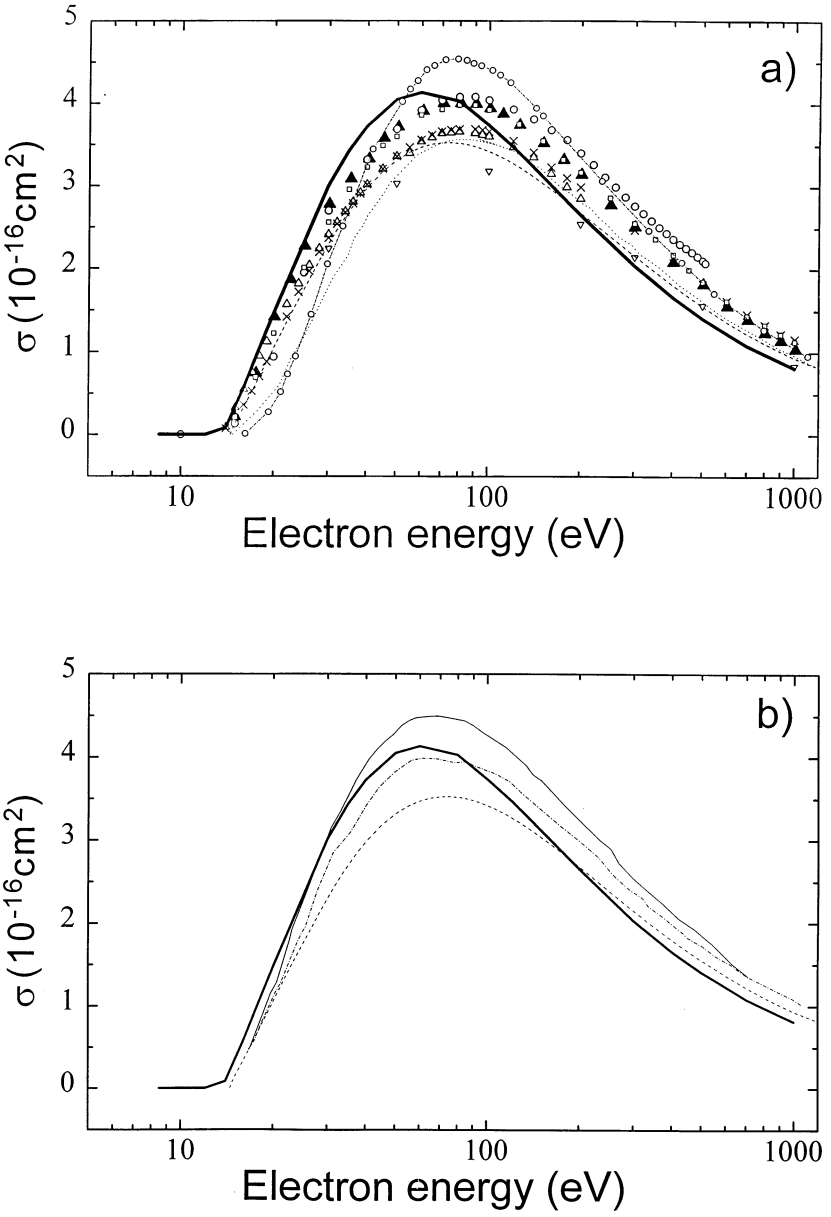

Fig. 2. Electron impact ionization cross section of CH_4 as a function of electron energy. (a) The experimental data points are from [89] (filled triangles), [88] (open circles), [90] (open triangles), [91] (crosses), [92] (inverted open triangles), and [93] (open squares). The thick solid line represents the present DM calculation, the fine dotted line represents the calculation of Jain and Khare [24], the dash-dotted line combined with open circles denotes calculated values as given in [51] using the method of Saksena et al. [49], and the dashed line represents the recent BEB results from [28] using a vertical ionization energy. (b) The thin solid line and the dash-dotted line denote respectively the BED and BEB calculation as reported in [51], the thick solid line represents the present DM calculation, and the dashed line represents the recent BEB results from [28] using a vertical ionization energy.

being well known from both experiment and calculation.

CH_3, CH_2, CH: The free radicals CH_x ($x = 1–3$) are readily produced by dissociation of methane in collisions with charged particles and photons. Because of the difficulty of producing well-characterized beams or static gas targets of these radicals for collision experiments, ionization cross section data for CH_x ($x = 1–3$) are scarce. The ionization cross section measurements by Baiocchi et al. [95] in CD_2 and CD_3 were the first ever reported ionization cross section measurements of free radicals. These authors employed the fast-neutral-beam technique that is particularly suited for ionization studies involving free radicals. Tarnovsky et al. [96] subsequently carried out a more comprehensive series of ionization cross section measurements for all four CD_x ($x = 1–4$) targets using the same experimental technique in a somewhat improved apparatus (in terms of its ability to detect energetic fragment ions with 100% efficiency for all but the lightest fragment ions [96,97]). We note that both experimental studies were carried out using the deuterated (CD_x) rather than the protonated (CH_x) targets that made it easier to separate the various fragment ions resulting from a particular parent molecule [96,97]. Ionization cross sections are insensitive to isotope effects to a very high degree of approximation [98–100]. Fig. 3 shows the experimentally determined ionization cross sections for CH_x in comparison with the present calculations and the BEB calculation of Kim and co-workers [27]. In the case of the CH radical (Fig. 3, top), the only experimental data of Tarnovsky et al. [96] are described quite well by both calculations for energies below about 30 eV, whereas the experimental data at higher impact energies lie below both calculations (which agree very well with one another over the entire range of impact energies). A possible explanation for this discrepancy could be the fact that the H^+ fragment ions that are formed with a significant amount of kinetic energy are not detected efficiently in the experiment of Tarnovsky et al. [96]. In the case of CH_2 (Fig. 3, center), the early data of Baiocchi et al. [95] lie systematically below both calculations and below the data reported by Tarnovsky et al. [96], which include estimates for those energetic fragment ions that might not have been detected with 100% efficiency in their experiment. The present calculations lie somewhat above the BEB calculations and the experimental data of Tarnovsky et al. [6], but are consistent with the experimental data within the quoted experimental error of 20%. A similar situation is found for CH_3 (Fig. 3, bottom), where (1) the experimental data of Tarnovsky et al. [96] lie slightly above the data of Baiocchi et al. [95] and (2) the data of Tarnovsky et al. [96] are in excellent agreement with the BEB calculations and in very good agreement with the present calculation that lies slightly above the BEB calculations.

C_2H_6: In C_2H_6 (Fig. 4), there are four experimental data sets [90,101–103] that are in very good agreement with one another. The BEB calculation of Kim and co-workers [27] represents the experimental data quite well over the entire range of impact energies. The present calculation and the calculation by Jain and Khare [35], which agree well with one another over the entire energy range, overestimate the cross section in the region of maximum by about 10–15%, but agree well with all other data at low and high energies.

C_2H_2: Fig. 5 shows three sets of experimentally determined C_2H_2 ionization cross section curves [104–106] in comparison with a BEB calculation and with the present DM calculation. Both calculations are in good agreement with the experimental data of Gaudin and Hagemann [106] that lie somewhat below the cross section of Tate and Smith [105] and the very recent data reported by Zheng and Srivastava [104]. We note in particular the excellent agreement between the measured cross sections of Tate and Smith [105] and Zheng and Srivastava [104] that resulted from very different experimental techniques and were reported more than 60 years apart.

C_6H_6: Fig. 6 shows the experimental data set of Schram et al. [101] for C_6H_6 that are limited to high impact energies above 500 eV in comparison with the BEB calculation [27] and the present DM calculation. The single data point at 75 eV is from Lampe et al. [107]. The DM calculation lies systematically above the BEB calculation, particularly in the region of the

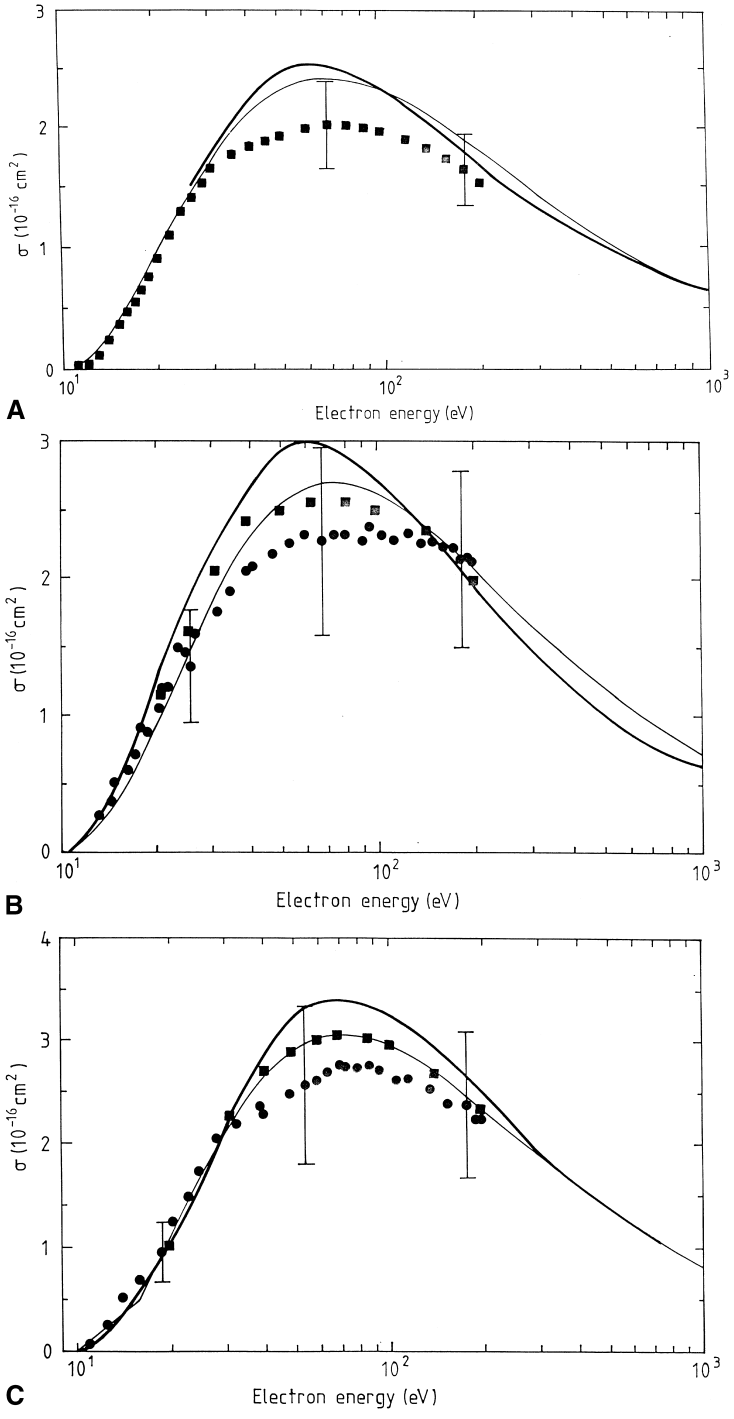

Fig. 3. Electron impact ionization of the CH_x (x = 1–3) free radicals as a function of electron energy. The thick solid line represents the present DM calculation and the thin solid line denotes the BEB calculation [27]. The experimental data points (taken for fully deuterated species) are from Baiocchi et al. [95] (full dots) and from Tarnovsky et al. [96] (full squares). Top diagram: CH. Center diagram: CH_2. Bottom diagram: CH_3.

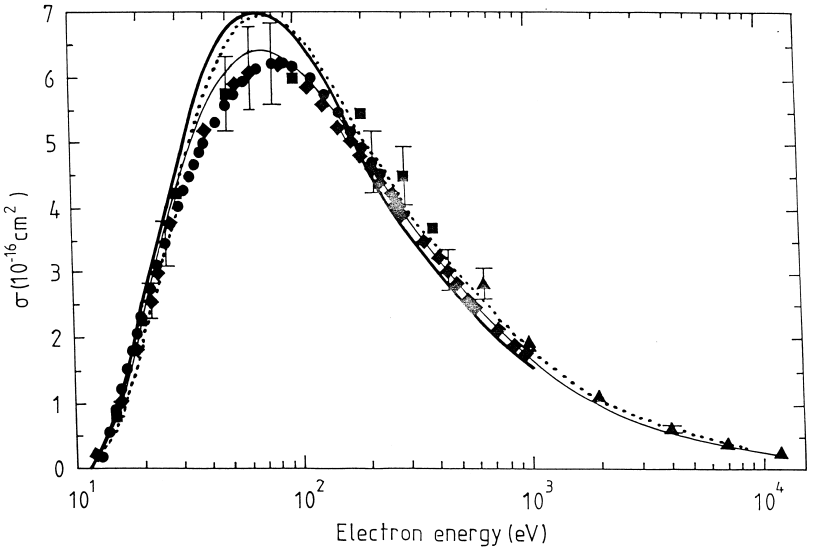

Fig. 4. Electron impact ionization cross section of C_2H_6 as a function of electron energy. The experimental data points are from [90] (filled circles), [103] (filled diamonds), [101] (filled triangles), and [102] (filled squares). The thick solid line represents the present DM calculation, the thin solid line denotes the BEB calculation [27], and the dotted line represents the calculation of Jain and Khare [35].

cross section maximum and is close to the single data point of Lampe et al. [107] at 75 eV. The experimental data of Schram et al. [101] appear to lie above the calculated cross sections except at very high energies close to 10 keV.

3.2. Selected fluorine-containing compounds (CF_x (x = 1–4), NF_x, SiF_x (x = 1–3), C_2F_6, SF_6)

Many fluorine-containing molecules have gained prominence in a variety of technological applications, most notably in the plasma-assisted processing of materials (fluorocarbons, nitrogen fluorides, and silicon fluorides) and gaseous dielectrics (SF_6).

CF_4: The carbon-tetrafluoride (CF_4) molecule is a frequently used compound in fluorocarbon plasmas that are widely used in the semiconductor industry, primarily for the etching of Si-based microelectronic devices. CF_4 also emerged as a "benchmark test" for experimental ionization studies in the sense that it was the first molecule where discrimination effects in the detection of energetic fragment ions were recognized as a possible source of major systematic uncertainties in the determination of dissociative ionization cross sections [108,109] in earlier experiments. In the past 10 years, there have been several experimental studies of the electron-impact ionization cross sections of CF_4 and there is now excellent agreement between the experimental data obtained by various groups using different experimental techniques [55,108–111] as shown in Fig. 7. Also shown in Fig. 7 are the results of the present calculations and three versions of the BEB calculations using different wave functions with and without estimates for multiple ionization processes as discussed in detail in [55]. The various BEB calculations and the present calculations are in very good agreement with each another and with the experimental data over the entire energy range from threshold to more than 1000 eV.

CF_3, CF_2, CF: The CF_x radicals are important secondary reaction products in fluorocarbon plasmas. These radicals are chemically very active and they are largely responsible for the plasma chemical gas phase and surface reactions in fluorocarbon plasmas. Fig. 8 shows the measured total single ionization cross sections for the CF_x (x = 1–3) free radicals of

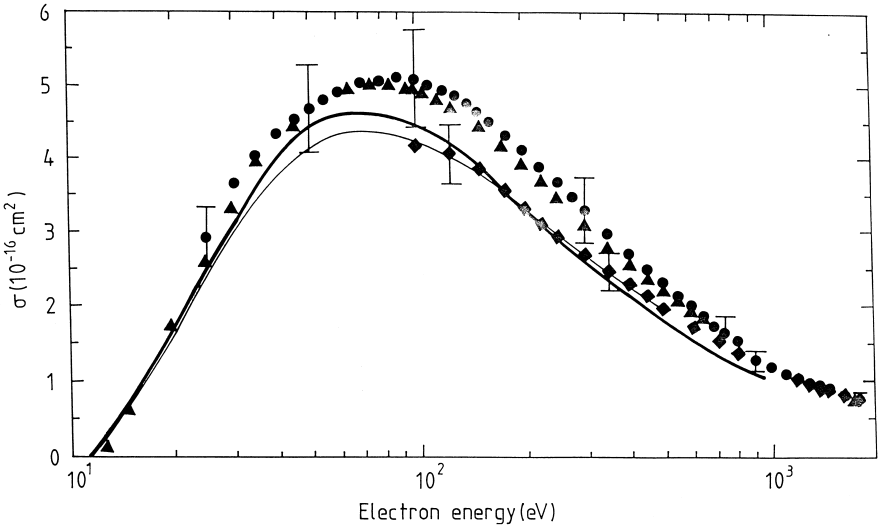

Fig. 5. Electron impact ionization cross section of C_2H_2 as a function of electron energy. The experimental data points are from [106] (filled diamonds), [104] (filled circles), and [105] (filled triangles). The thick solid line represents the present DM calculation and the thin solid line denotes the BEB calculation [27].

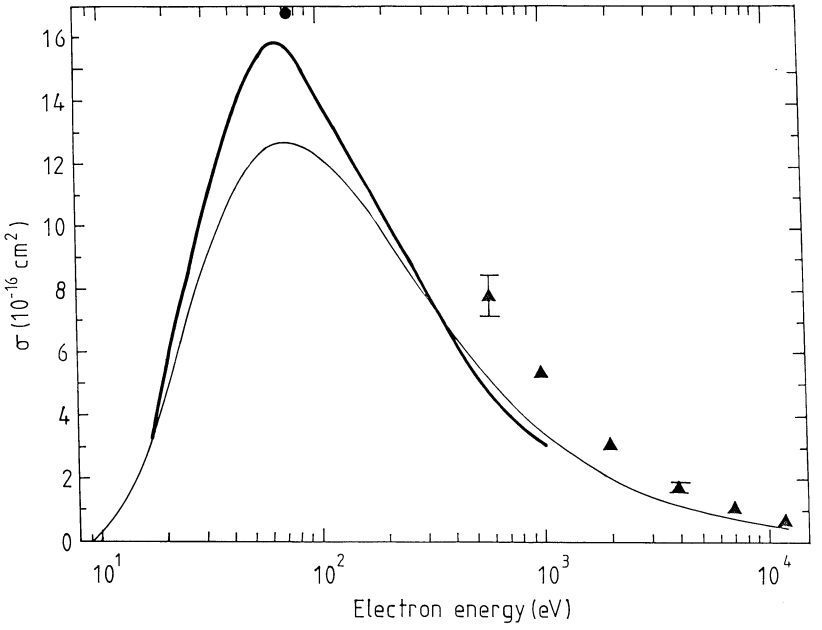

Fig. 6. Electron impact ionization cross section of C_6H_6 as a function of electron energy. The experimental data points are from [101] (filled triangles) and the single data point at 75 eV is from [107]. The thick solid line represents the present DM calculation and the thin solid line denotes the BEB calculation [27].

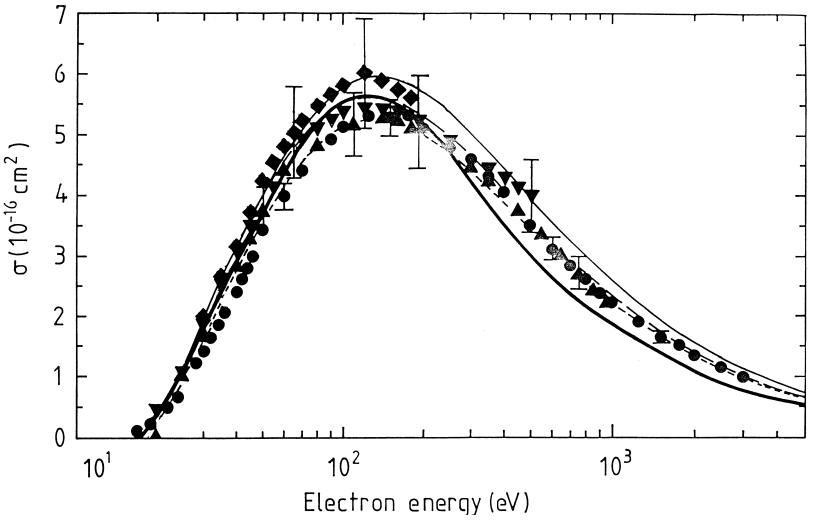

Fig. 7. Electron impact ionization cross section of CF_4 as a function of electron energy. The experimental data points are from [55] (filled circles), [108] (filled diamonds), [110] (filled triangles), [109] (filled inverted triangles), and [111] (filled squares). The thick solid line represents the present DM calculation, the thin solid line and the two dashed lines denote different variants of the BEB calculation [55] (i.e. thin solid line: CAS wave functions with estimate for multiple ionization; long dashed line: CAS wave functions without estimate for multiple ionization; short dashed line: RHF wave functions without estimate for multiple ionization).

Tarnovsky and Becker [112] and Tarnovsky et al. [113] in comparison with the present calculations. Even though the present calculations represent a slight improvement compared to the previous calculations for these targets of Deutsch et al. [17] that used an earlier variant of the DM formalism, there are still serious discrepancies between the measured and calculated cross sections. For all three targets, the calculations lie significantly (40–50%) above the measured data. There is no simple explanation for this level of disagreement, particularly in view of the excellent agreement between experiment and calculation in the case of CF_4 and CH_x (see above).

NF_3, NF_2, NF: Nitrogen trifluoride is widely used in the semiconductor industry for the cleaning of plasma reactors. The ionization and decomposition of the NF_3 molecule and the NF_2 and NF radicals have been investigated experimentally by two groups [114,115]. As shown in Fig. 9, the experimental cross sections from Tarnovsky et al. [114,115] lie below the calculated cross sections by as much as 50%. This finding is very similar to what was observed in the case of the CF_x radicals.

SiF_3, SiF_2, SiF: The SiF_x ($x = 1$–3) free radicals represent a group of species for which the measured total single ionization cross section shows an "inversion" in the sense that the cross section declines in magnitude as the target gets bigger from SiF to SiF_2 to SiF_3 as first observed by Freund and co-workers [116–118]. As pointed out earlier [22] this behavior is due to the strong ionic bonding of the F atoms and the very small atomic radius of the fluorine valence electrons. As a consequence, the dominant part of the molecular ionization cross section comes from the valence electrons of the Si atom that has a much larger ionization cross section than atomic fluorine ("shielding effect"). When Si and F combine to form SiF, one of the four valence electrons of Si is transferred to F and the SiF ionization cross section is determined largely by the remaining three Si valence electrons. In SiF_2, two Si valence electrons remain, causing the ionization cross section to decline. Likewise, the SiF_3 cross section declines further because there is only a single Si valence electron left. Fig. 10 shows the measured SiF_x ionization cross sections in comparison with the present calculations and with two vari-

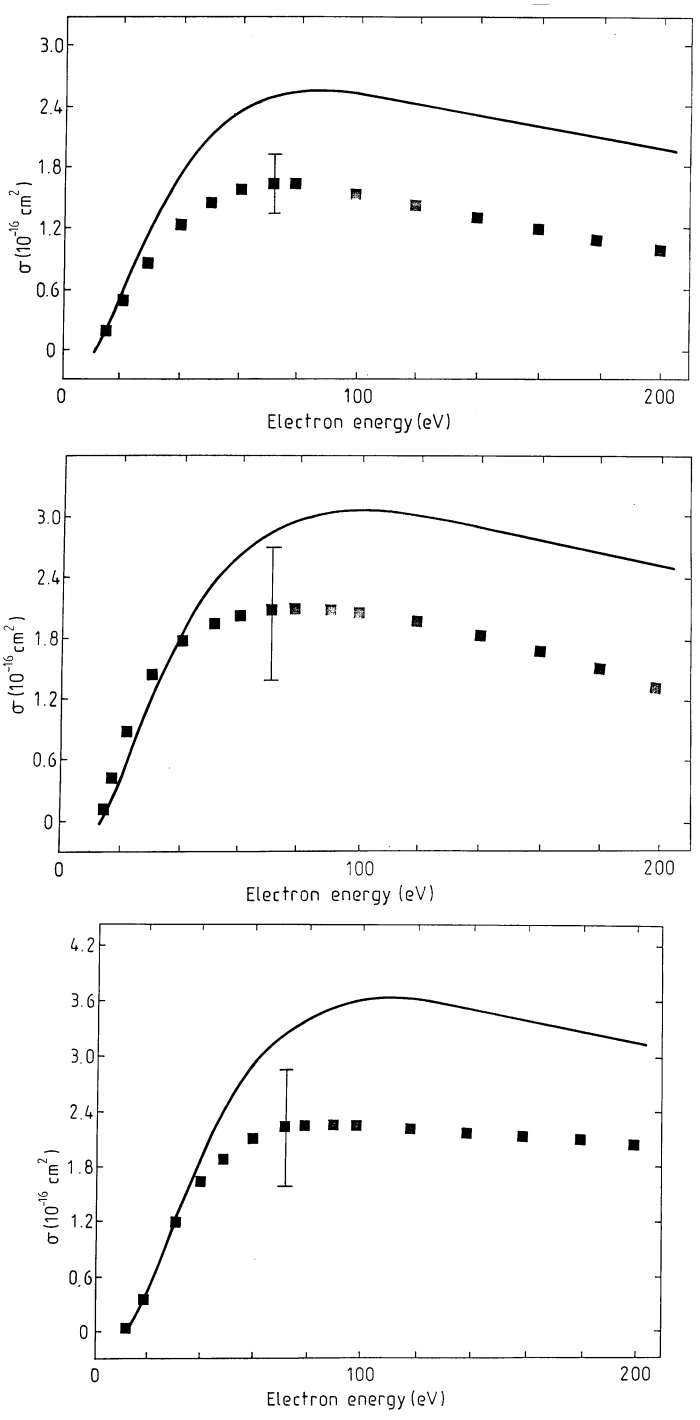

Fig. 8. Electron impact ionization of the CF_x (x = 1–3) free radicals as a function of electron energy. The thick solid line represents the present DM calculation. The experimental data points are from Tarnovsky et al. [112,113] (filled squares). Top diagram: CF. Center diagram: CF_2. Bottom diagram: CF_3.

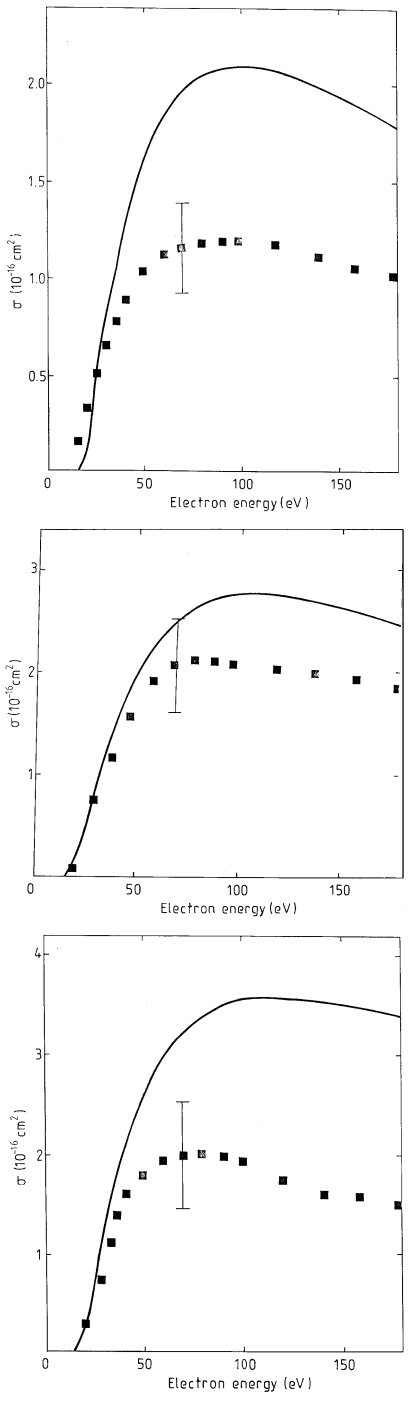

Fig. 9. Electron impact ionization of the NF_x (x = 1–3) compounds as a function of electron energy. The thick solid line represents the present DM calculation. The experimental data points (filled squares) are from Tarnovsky et al. [114,115]. Top diagram: NF. Center diagram: NF_2. Bottom diagram: NF_3.

ants of the BEB calculations [27]. For all three targets, the present calculations agree best with the so-called "BEB/3" calculation [27], whereas the "BEB" calculation [27] lies somewhat below the other two calculated cross section curves. We observe a systematic trend as far as the agreement between measured and calculated cross sections is concerned from (1) a measured cross section that exceeds the calculated cross section for SiF, to (2) satisfactory agreement between experiment and calculation for SiF_2, to (3) calculated cross sections that exceed the measured cross section for SiF_3. However, the discrepancies between measured and calculated cross sections in the case of SiF and SiF_3 are not nearly as severe as what was observed for CF_x and NF_x (x = 1–3).

C_2F_6: Next to CF_4, C_2F_6 is the most frequently used fluorocarbon compound in plasma processing applications. Fig. 11 shows the measured C_2F_6 ionization cross sections of Nishimura et al. [55], Poll and Meichsner [119], Beran and Kevan [111], and Kurepa [120] in comparison with the same three variants of the BEB calculation [55] that were employed for CF_4 and with the present DM calculation. The BEB calculation using CAS wave functions with estimates for multiple ionization processes shows the best overall agreement with the experimental data, except perhaps with the data of Poll and Meichsner at energies above ~60 eV, where the data reported by these authors lie systematically below all other experiments (very likely due to discrimination effects inherent to this experiments, see [108]). The present DM calculation lies consistently below all experimental data and the deviation increases with increasing impact energy. Above ~100 eV, the DM calculation underestimates the experimental data by as much as 25%.

SF_6: SF_6 is another important fluorine-containing molecule because of its use in gaseous dielectrics. Fig. 12 shows the experimentally determined SF_6 ionization cross sections of Rapp and Englander-Golden [91] and Margreiter et al. [121] in comparison with the BEB calculation of Kim and co-workers [27] and the present DM calculation. The two experimental data sets, which are in excellent mutual agreement agree well with both calculations up to about 30 eV,

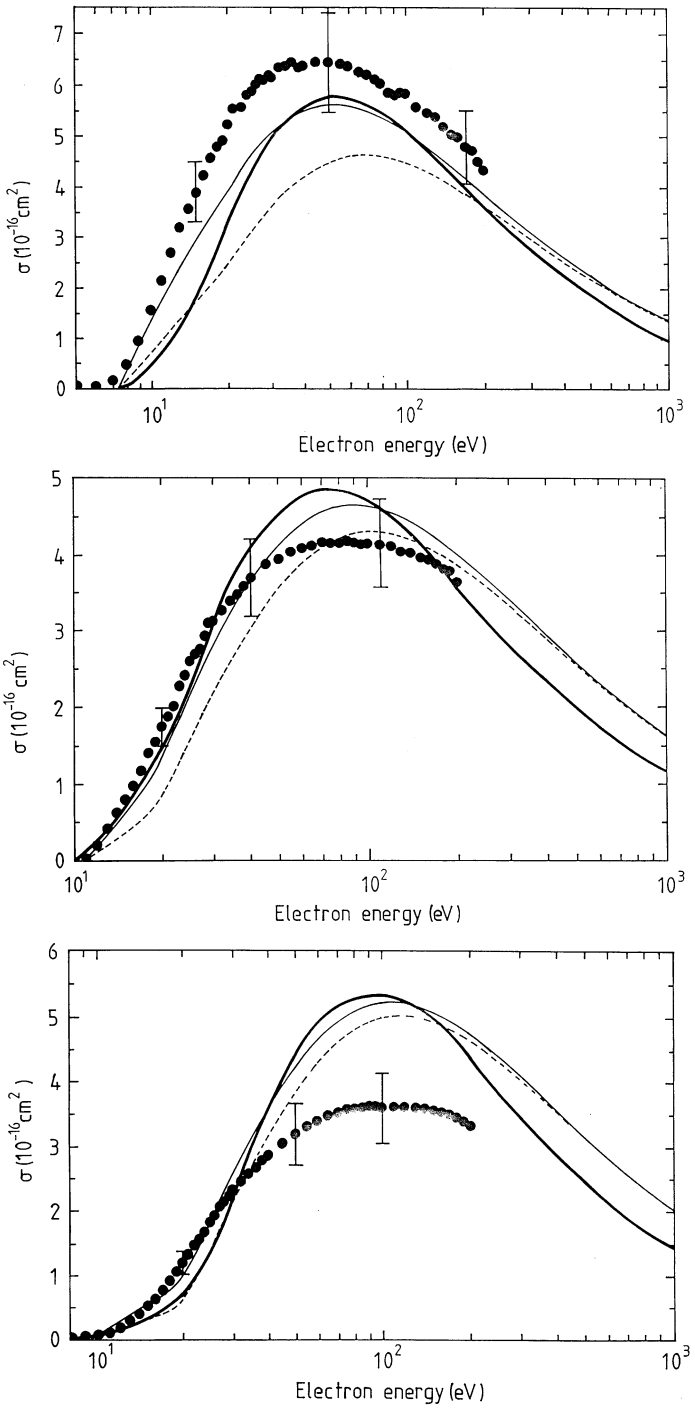

Fig. 10. Electron impact ionization of the SiF_x ($x = 1–3$) free radicals as a function of electron energy. The thick solid line represents the present DM calculation, the thin solid line and the dashed line denote two variants of the BEB calculation [27] (see text for details). The experimental data points (filled circles) are from Freund and co-workers [116–118] (full dots). Top diagram: SiF. Center diagram: SiF_2. Bottom diagram: SiF_3.

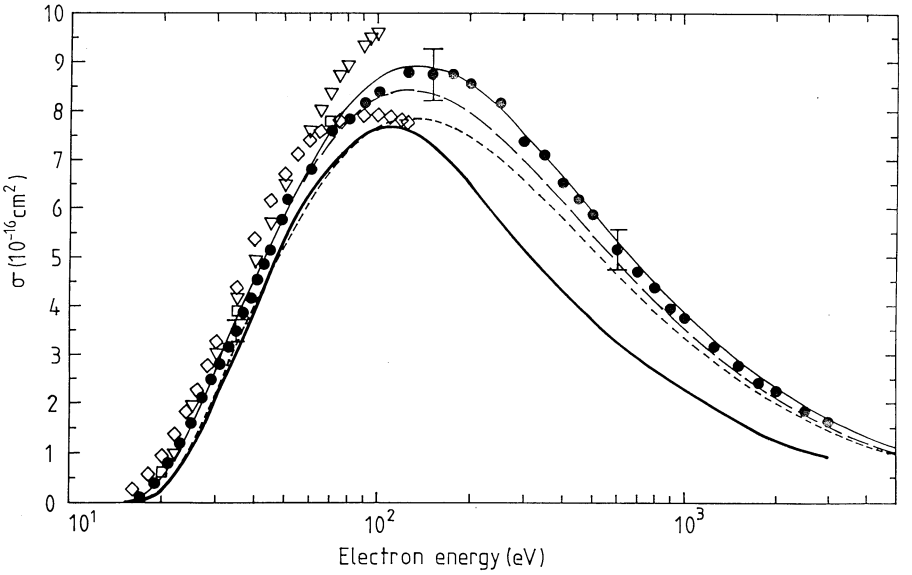

Fig. 11. Electron impact ionization cross section of C_2F_6 as a function of electron energy. The experimental data points are from [120] (open inverted triangles), [55] (filled circles), [111] (open squares), [119] (open diamonds). The thick solid line represents the present DM calculation, the thin solid line and the two dashed lines denote different variants of the BEB calculation [55] (see caption of Fig. 7 for details).

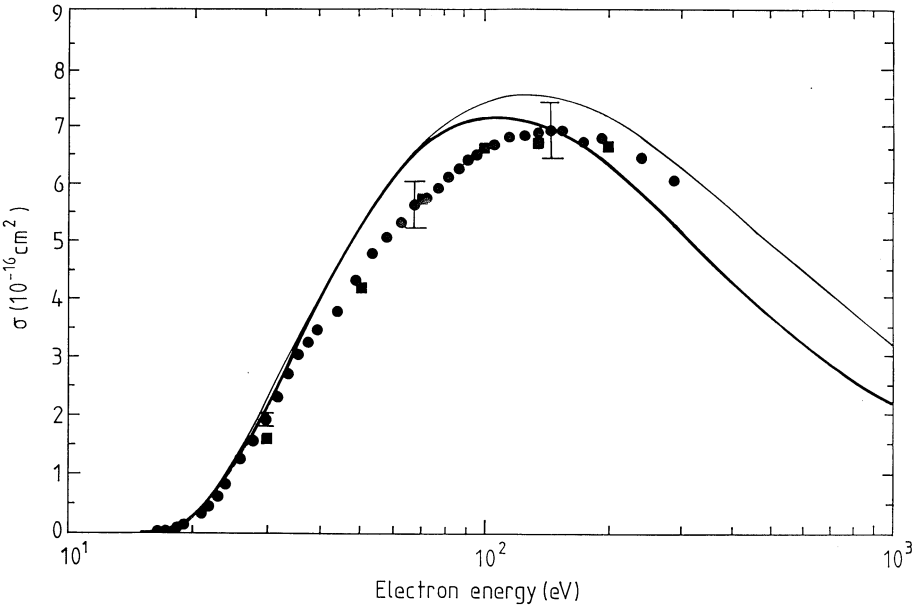

Fig. 12. Electron impact ionization cross section of SF_6 as a function of electron energy. The experimental data points are from [91] (filled squares) and [121] (filled circles). The thick solid line represents the present DM calculation and the thin solid line denotes the BEB calculation [27].

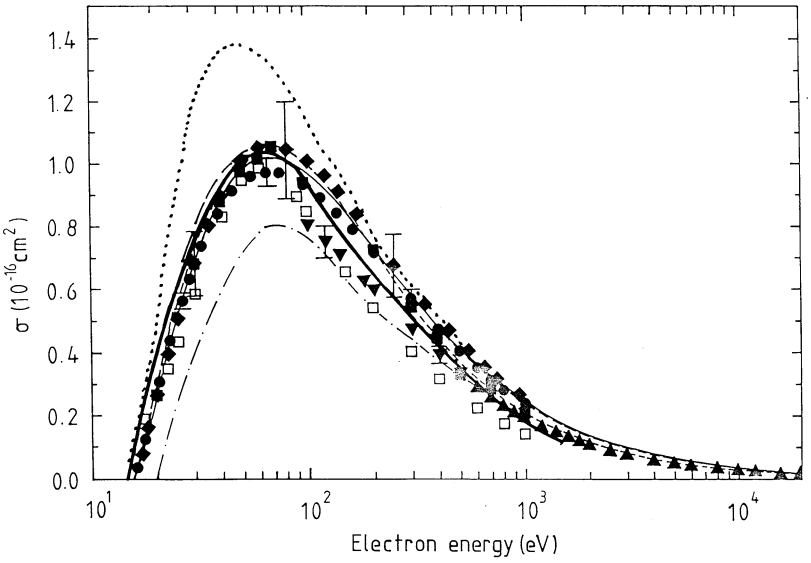

Fig. 13. Electron impact ionization cross section of H_2 as a function of electron energy. The experimental data points are from [126] (filled squares), [91] (filled circles), [125] (filled diamonds), [123] (filled triangles), and [124] (filled inverted triangles). The open squares denote CTMC calculations of [128]. The thick solid line represents the present DM calculation, the thin solid line and the dashed line denote the BEB and BED calculation, respectively [27], the dash-dot line is the calculation of Saksena et al. [49], and the dotted line denotes results obtained with the method of Khare and co-workers [127].

but fall below both calculated curves between 30 and ~100 eV. Both experimental cross sections reach their maximum at impact energies that are somewhat higher than the peak in the two calculated cross section curves. At higher impact energies, the DM cross section appears to decline faster than the two measured cross sections and the BEB cross section. Recently, the BEB results have been revised [122] to include multiple ionization. The multiple ionization shifts the peak position to higher incident energy and that leads to a very good agreement with the shape of the cross section curve reported by Rapp and Englander-Golden [91]; nevertheless the new BEB cross section values are about 17% above the experimental values [91].

3.3. Diatomic molecules (H_2, N_2, O_2, S_2, C_2), C_3, and ozone (O_3)

The homonuclear diatomic and triatomic molecules listed above represent the simplest molecular targets and most of them have been studied extensively because of their basic relevance in electron–molecule collision physics and because of their relevance in applications ranging from planetary and cometary atmospheres to gas discharges, plasmas, and combustion processes.

H_2: The electron-impact ionization of H_2, which is the simplest neutral molecule, has been studied experimentally by several groups. Fig. 13 shows the measured H_2 ionization cross sections of Rapp and Englander-Golden [91], Schram et al. [123,124], Krishnakumar and Srivastava [125], and Straub et al. [126] in comparison with the calculated BEB cross sections as well as with the more rigorous BED cross sections of Kim and co-workers [27], the cross section of Saksena et al. [49], the cross section of Khare and co-workers [127], and the present DM cross section. There is excellent agreement among the various experimental data sets as well as between the measured cross sections and the calculated DM, BEB, and BED cross sections from threshold to 10 keV. The

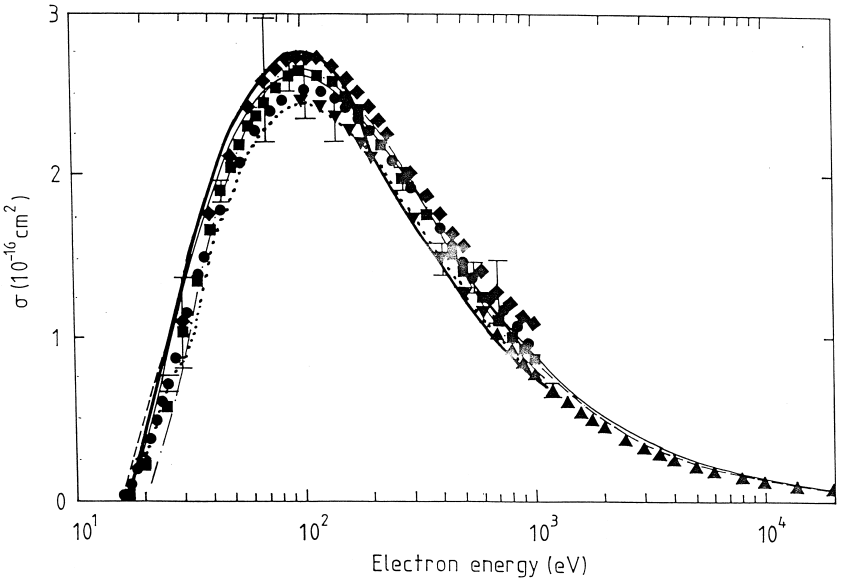

Fig. 14. Electron impact ionization cross section of N_2 as a function of electron energy. The experimental data points are from [126] (filled squares), [91] (filled circles), [125] (filled diamonds), [123] (filled triangles), and [124] (filled inverted triangles). The thick solid line represents the present DM calculation, the thin solid line and the dashed line denote the BEB and BED calculations, respectively [27], the dash-dot line represents the calculation of Saksena et al. [49], and the dotted line denotes results obtained with the method of Khare and co-workers [127].

open squares denote the classical trajectory Monte Carlo (CTMC) calculation of Schultz et al. [128] that agrees well with the experimental data up to ~100 eV. The cross section calculated by Saksena et al. [49] on the basis of the extended method of Khare and co-workers disagrees with all other cross sections in the regime of lower impact energies up to ~400 eV. The cross section of Khare and co-workers [127], on the other hand, overestimates all other cross sections for energies from 20 to 300 eV and, in particular, in the region of the cross section maximum.

N_2: Molecular nitrogen, N_2, is another example where various measured cross sections reported by different authors over a period of more than 20 years are in excellent agreement with one another as well as with calculated cross sections on the basis of the BEB, BED [27], and DM formalism (see Fig. 14). In contrast to the case of H_2, the calculated N_2 cross sections of Saksena et al. [49] and Khare and co-workers [127] are in excellent agreement with all other cross sections over the entire range of impact energies.

O_2: The situation is somewhat less satisfactory for molecular oxygen, O_2 (see Fig. 15). The agreement among the various measured cross section data is good, but not nearly as good as for H_2 and N_2, particularly in the region of the cross section maximum. The calculated BEB cross section [27] is in excellent agreement with the experimental data of Straub et al. [126] and Schram et al. [123,124]. The calculated cross section of Saksena et al. [49] does not describe the region of the maximum in the cross section curve very well, whereas the cross section calculated on the basis of the method of Khare and co-workers [127] lies consistently below the experimental data. The DM calculation represents the measured data quite well up to energies of about 50 eV, but underestimates the measured data at higher impact energies by as much as 25%. In fact, above 100 eV, the DM cross section lies even below the cross section of [127]. We have no simple explanation for this level of disagreement in the case of O_2.

S_2: Fig. 16 shows the experimentally determined ionization cross section of Freund et al. [129] for S_2 in

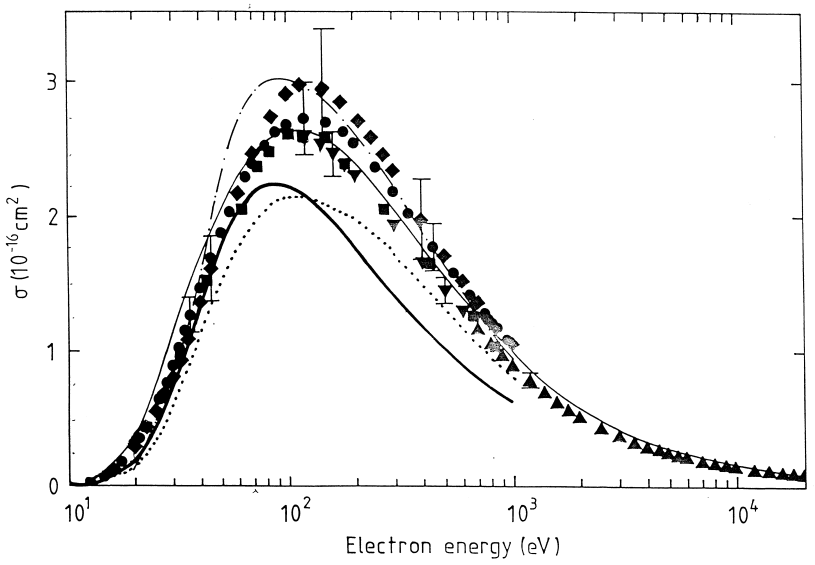

Fig. 15. Electron impact ionization cross section of O_2 as a function of electron energy. The experimental data points are from [126] (filled squares), [91] (filled circles), [125] (filled diamonds), [123] (filled triangles), and [124] (filled inverted triangles). The thick solid line represents the present DM calculation, the thin solid line denotes the BEB calculation [27], the dash-dot line shows the calculation of Saksena et al. [49], and the dotted line denotes the results obtained with the method of Khare and co-workers [127].

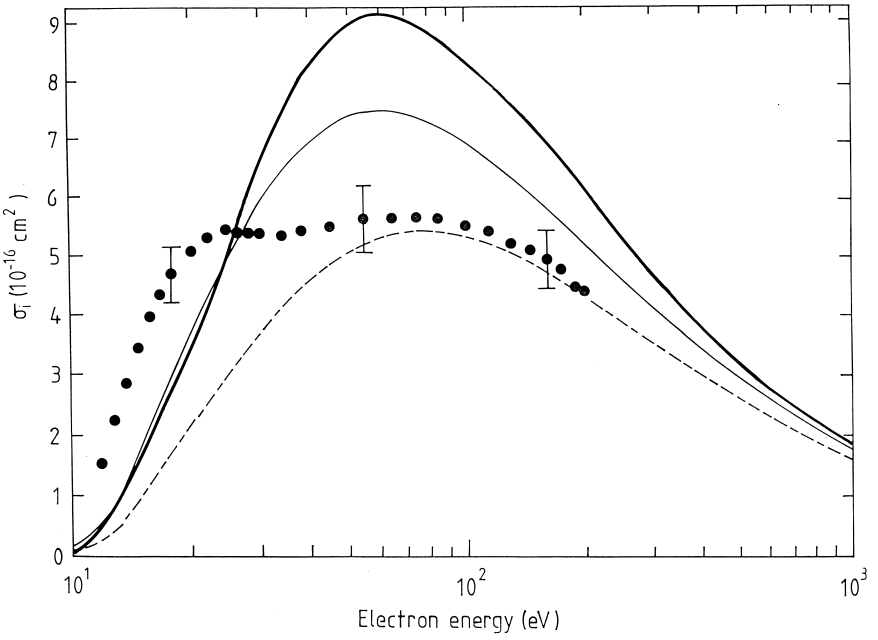

Fig. 16. Electron impact ionization cross section of S_2 as a function of electron energy. The experimental data points are from [129] (filled circles). The thick solid line represents the present DM calculation. The thin solid line and the dashed line denote two variants of the BEB calculation [28].

comparison with two variants of the BEB method, a "U/3" calculation and a standard "U" calculation (see [28] for details) and the present DM calculation. None of the calculated cross sections describes the experimental data that exhibit a peculiar double-maximum structure with one maximum at very low impact energies around 20 eV and a second maximum at around 70 eV that is more typical for molecular ionization cross section curves. The "standard" BEB calculation appears to provide a reasonable description of the experimental data at higher energies, above ~70 eV. We note that the experimental S_2 cross section data are in the region of the maximum only ~20% above that of the atomic S cross section data measured by the same authors [129].

C_2, C_3: Fig. 17 shows calculated DM ionization cross sections for the carbon dimer (C_2) and the carbon trimer (C_3) for which there are no experimental data at this time. The calculations utilized three [C_2, Fig. 17(a)] or two [C_3, Fig. 17(b)] different atomic basis sets (6-311G, cc-pVDZ, and, in the case of C_2, also STO-6G). It is obvious from the C_2 calculations that the ionization cross sections based on the cc-pvdz and 6-311G basis sets yield essentially identical results, whereas the calculation using the simpler STO-6G basis sets results in a cross section that has an unrealistically low threshold, a larger peak cross section value at a lower impact energy, but a similar high-energy dependence. In the case of C_3, we limited the calculations to the cc-pVDZ and 6-311G atomic basis sets that lead to essentially identical cross section curves with the expected spectroscopic ionization threshold [130].

O_3: Fig. 18 shows two experimental data sets for O_3: the absolute cross sections measured by Siegel [131] and the relative cross section measurement of Newson et al. [132] that these authors normalized to the absolute cross section of Siegel. Also shown in Fig. 18 are the calculated BEB [28] and DM cross sections that both overestimate the experimental data, particularly in the region of the cross section maximum. Overall, the DM cross section is closer to the experimental data than the BEB cross section. We note that the O_3 experimental cross section data are essentially of the same magnitude as the O_2 experimental cross section data.

3.4. Other molecules (H_2O, NH_3, CO_2, CH_3OH, $TiCl_4$)

The molecules H_2O, NH_3, and CO_2 are abundant constituents of many environments. The ionization properties of these molecules play an important role in many diverse applications ranging from planetary atmospheres to radiation chemistry. Ionization cross sections for these abundant and important molecules have been measured over the past 60 years by many groups using various experimental techniques. The reliability and quality of the many published data sets ranges from poor to very high. Similar to what was done earlier in the case of CH_4 (see earlier discussion) we limited the number of data sets shown for these three molecules in Figs. 19–21 to a few data sets using selection criteria similar to those applied earlier to CH_4.

H_2O: Fig. 19 shows four selected sets of measured ionization cross sections for H_2O [133–136] in comparison with the present DM calculation, a BEB calculation [27], a calculation by Khare and coworkers [24], and a more recent calculation by Saksena et al. [49] using a variant of the formalism of Khare and collaborators [24]. There is good agreement among the four experimental data sets within their combined margins of uncertainty. All four calculated cross section curves are in good agreement with one another and also in good agreement with the experimental data from threshold to 1000 eV.

NH_3: Fig. 20 shows the experimental NH_3 ionization cross section data sets of Rao and Srivastava [137], Djuric et al. [47], Bederski et al. [138], and Crowe and McConkey [139] in comparison with four calculated cross sections that use the same methods as before in the case of H_2O (Fig. 19). The experimental data of [47, 137, 138] are in excellent agreement with one another and in reasonably good agreement with the data of Crowe and McConkey [139] whose cross section appears to rise somewhat faster than the cross

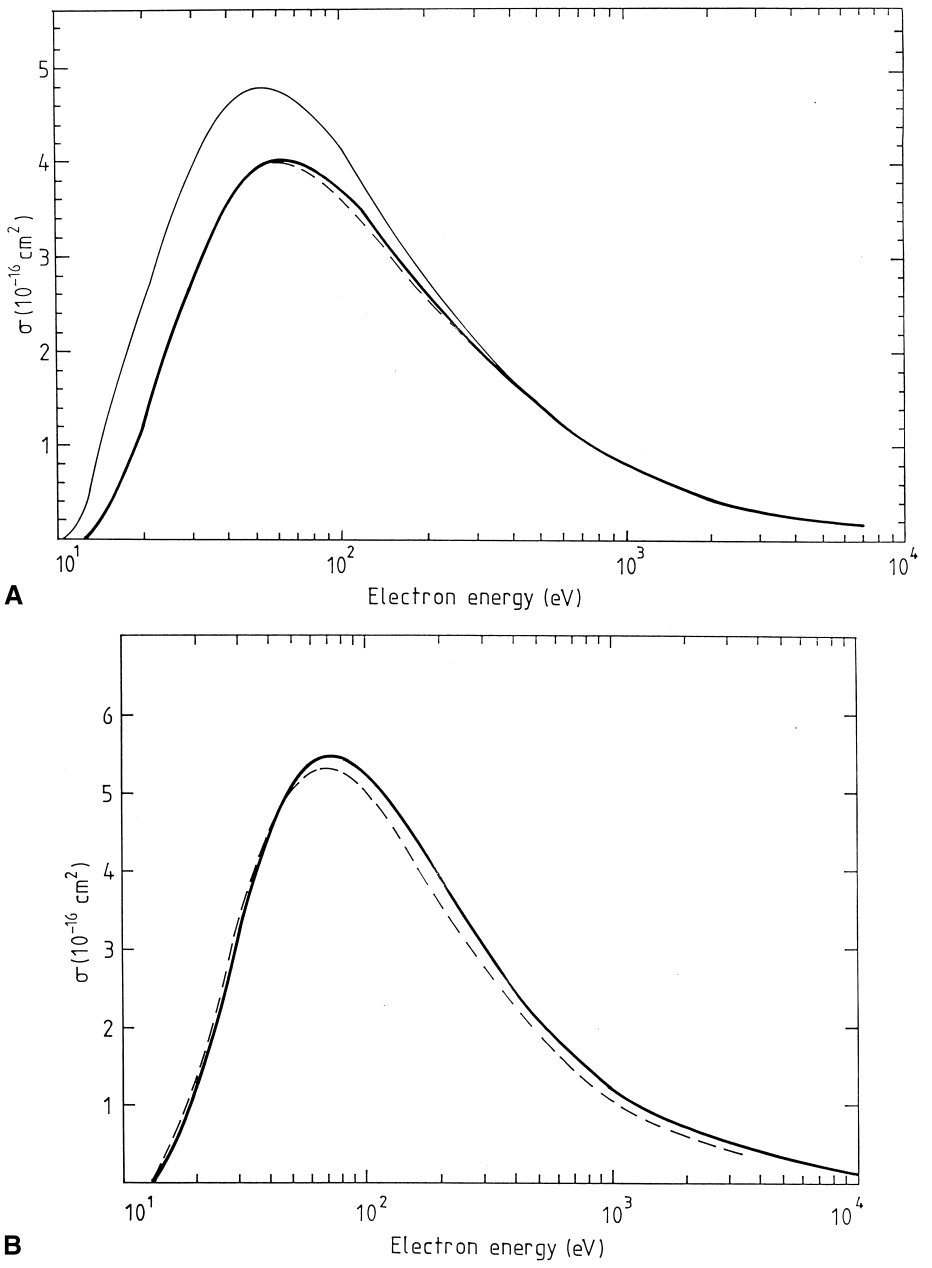

Fig. 17. Electron impact ionization cross section of C_2 and C_3 as a function of electron energy. (a) C_2: the three different curves represent DM calculations using three different atomic basis sets—6-311G (thick solid line), dashed line (cc-pVDZ), thin solid line (STO-6G). (b) C_3: the two different curves represent DM calculations using two different atomic basis sets—6-311G (thick solid line), dashed line (cc-pVDZ).

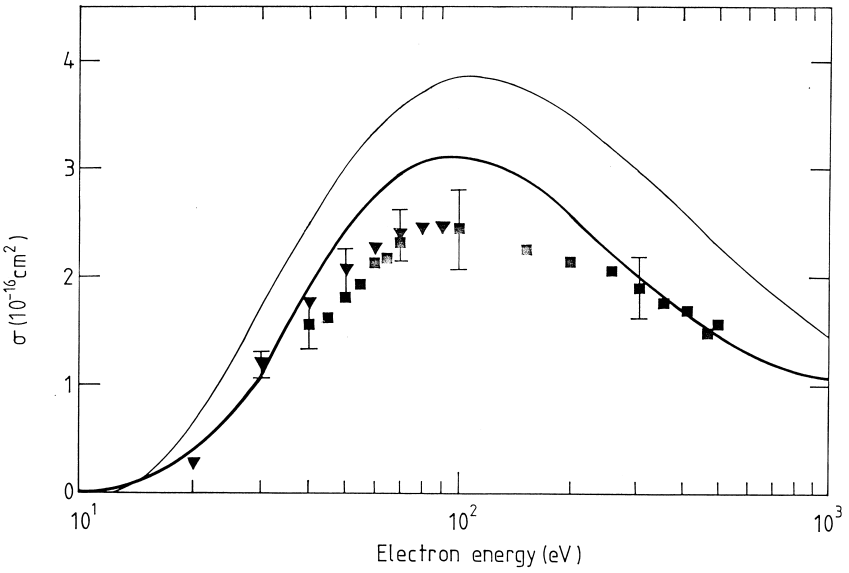

Fig. 18. Electron impact ionization cross section of O_3 as a function of electron energy. The experimental data points from [132] (filled squares) are normalized to the absolute measurements of [131] (filled inverted triangles). The thick solid line represents the present DM calculation and the thin solid line denotes the BEB calculation [28].

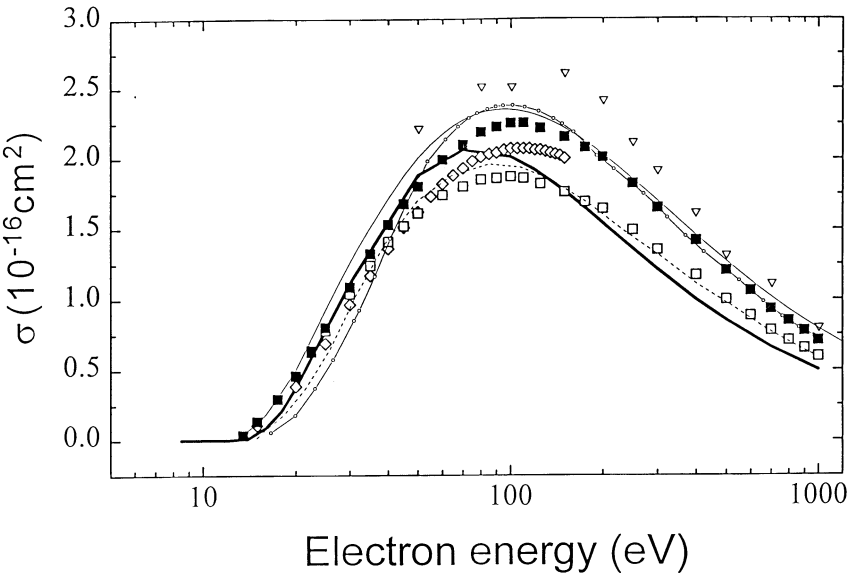

Fig. 19. Electron impact ionization cross section of H_2O as a function of electron energy. The experimental data points are from [136] (filled squares), [133] (open diamonds), [134] (open inverted triangles), and [135] (open squares). The thick solid line represents the present DM calculation, the thin solid line denotes the BEB calculation [27], the dashed line refers to the calculation of Khare and co-workers [24], and the open circles connected by a solid line denote the calculation of Saksena et al. [49].

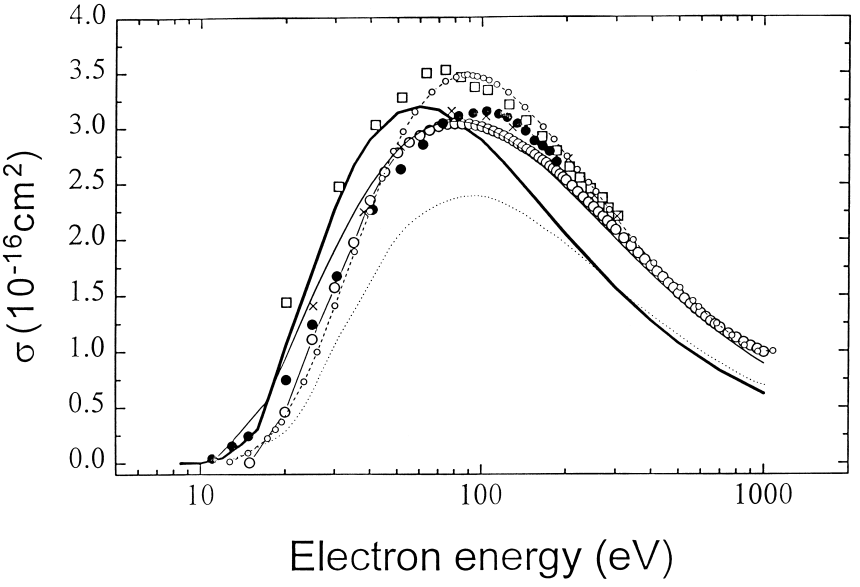

Fig. 20. Electron impact ionization cross section of NH_3 as a function of electron energy. The experimental data points are from [139] (open squares), [47] (filled circles), [137] (open circles), and [138] (crosses). The thick solid line represents the present DM calculation, the thin solid line denotes the BEB calculation [27], the dotted line refers to the calculation of Khare and co-workers [24], and the open circles connected by a dashed line denote the calculation of Saksena et al. [49].

section functions reported by the other groups. The calculated BEB cross section [27] and the calculation of Jain and Khare [24] show the best agreement with the data of [137,138,47], whereas the DM cross section is in better agreement with the data of Crowe and McConkey [139] in the energy regime from threshold to ~50 eV. Above 50 eV, the DM cross section declines faster than all experimental data and the other two calculated cross sections. The cross section calculated by Saksena et al. [49] lies systematically below all other calculated and measured data except perhaps at very low impact energies. An improved variant of the Khare et al. calculation (not shown in Fig. 20) carried out by Djuric et al. [47] gives a better agreement with the data of [47].

CO_2: Fig. 21 shows four selected data sets for CO_2 [51, 88, 140, 141] in comparison with four calculated cross sections that use the same methods as before in the case of H_2O (Fig. 19). All four experimental data sets agree with one another within their stated accuracy and all four calculations describe the measured cross sections quite well over the entire range of electron energies, except that the DM cross section again appears to decline faster than the other cross section curves in the high-energy region.

CH_3OH: Fig. 22 shows the measured CH_3OH cross section of Djuric et al. [142] in comparison with the present DM calculation. Although there is reasonable agreement between the measured and the calculated cross section in terms of the magnitude of the cross section, there is a serious disagreement as far as the cross section shape as a function of impact energy is concerned. The calculated cross section reaches its maximum at a much lower energy and declines faster toward higher impact energies compared to the measured cross section.

$TiCl_4$: Fig. 23 shows the recent measurement of the ionization cross section of the molecule titanium tetrachloride ($TiCl_4$) that is the precursor in the plasma-assisted deposition of technologically impor-

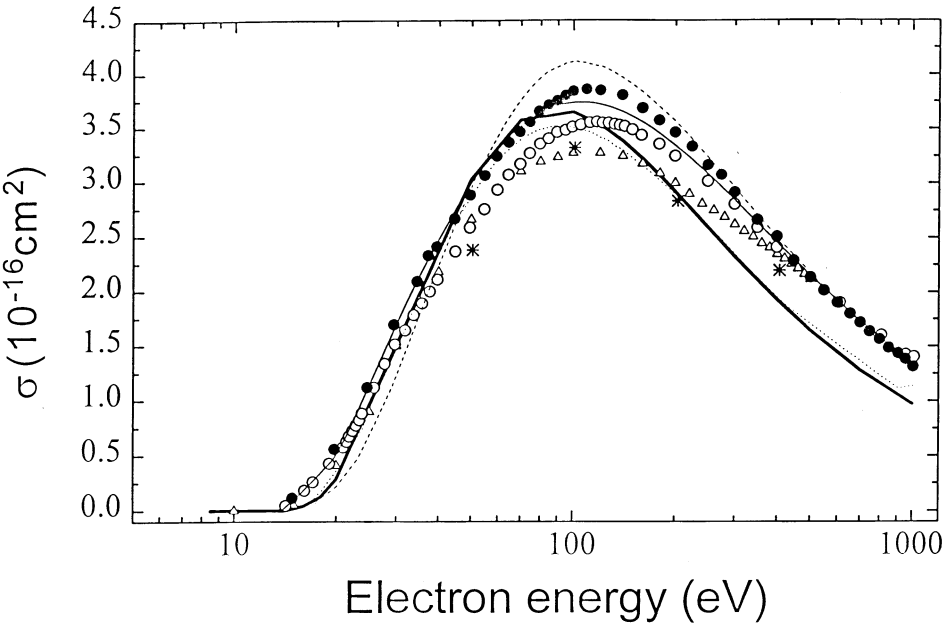

Fig. 21. Electron impact ionization cross section of CO_2 as a function of electron energy. The experimental data points are from [140] (filled circles), [91] (open circles), [141] (stars), and [88] (open triangles). The thick solid line represents the present DM calculation, the thin solid line denotes the BEB calculation [27], the dotted line represents the calculation of Jain and Khare [24], and the dashed line denotes the calculation of Saksena et al. [49].

tant TiN films. The total $TiCl_4$ ionization cross section is obtained from a complete set of partial ionization cross section measurements [143] and is compared to the present DM calculation, which represents the experimental data quite well, except in the region of the cross section maximum. The structure in the measured data around 50 eV could be the result of unusually prominent ion-pair formation processes contributing to one or more of the measured partial ionization cross sections. Ion-pair formation processes generally have very small cross sections for most molecules. Evidence for the presence of ion-pair formation channels has been found in molecules such as O_2, CO_2, C_2H_2, and in particular in halogen-containing molecules [144]. However, even in CF_4, which is known to have some of the largest cross sections for molecular ion-pair formation processes [145], the cross sections for ion-pair formation channels do not exceed a few percent of the direct ionization cross section. Ion-pair formation processes as well as indirect ionization processes are not included in the DM formalism, which is restricted to processes in which a single target electron is ejected into a direct ionization process.

4. Conclusion

Progress in the experimental determination of cross sections for the electron-impact ionization of molecules in the past decade served as a stimulus to revisit the state of theoretical calculations of molecular electron-impact ionization cross sections. In addition to the advancement of simplistic additivity rules and other simple calculational schemes, more rigorous methods have also gained prominence recently. More rigorous approaches in this context refer to methods that incorporate quantum mechanically calculated molecular structure information. This topical review summarizes recent developments in the appli-

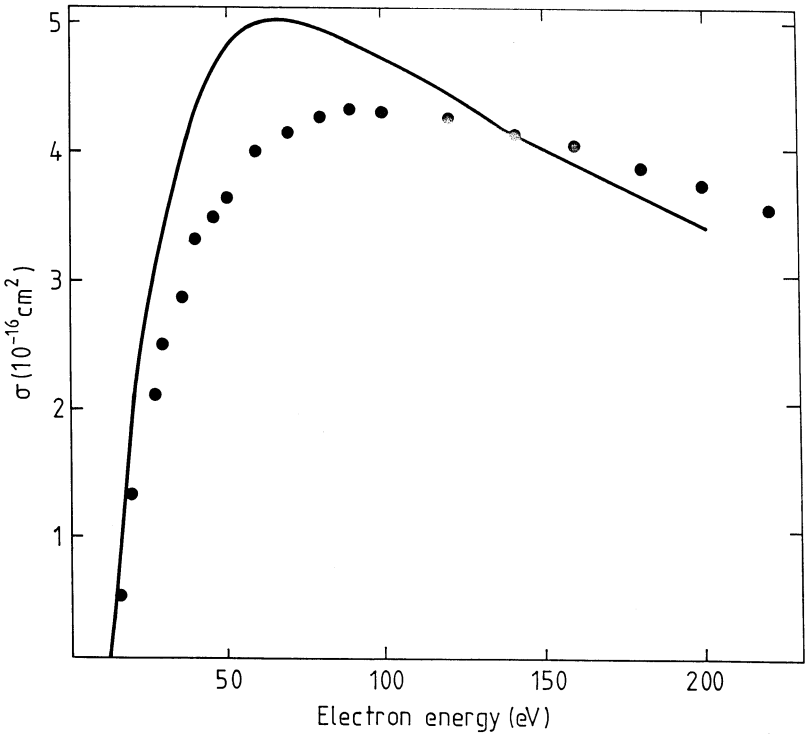

Fig. 22. Electron impact ionization cross section of CH_3OH as a function of electron energy. The experimental data points are from [142] (filled dots) and the thick solid line represents the present DM calculation.

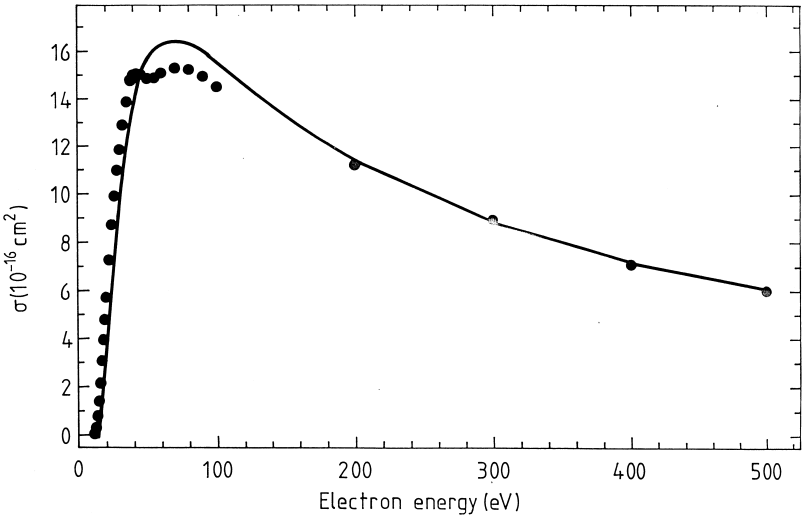

Fig. 23. Electron impact ionization cross section of $TiCl_4$ as a function of electron energy. The experimental data points are from [143] (filled dots) and the thick solid line represents the present DM calculation.

cation of three more rigorous approaches to the calculation of molecular ionization cross sections, viz. the method of Khare and co-workers, the approach of Kim and Rudd, and the DM formalism. All these approaches have been refined several times over the past few years. In this review, we compare the predictions of the most recent variants of these methods with available (and in certain cases critically evaluated) experimentally determined ionization cross section data. In most cases, there is very good to at least satisfactory agreement between the experimental data and the calculated data and among the calculated data. The most notable exceptions include the fluorine-containing species CF_x and NF_x ($x = 1–3$) where the DM calculation as well as preliminary results from the BEB approach [146] overestimate the measured data by as much as 50%.

Both the DM formalism and the BEB approach are comparatively straightforward calculation schemes that rely on information and data that are for the most either readily available in published literature or easily obtainable from standard quantum chemistry codes. This will help facilitate the incorporation of calculated ionization cross sections into cross section data sets of molecules for modeling codes and other applications and will enable comparisons with the rapidly increasing number of experimentally determined molecular ionization cross sections.

Acknowledgements

This work has been carried out within the Association EURATOM-ÖAW and was partially supported by the FWF, ÖNB, BMWV, Wien, Austria. One of us (KB) acknowledges partial financial support from the Division of Chemical Sciences, Office of Basic Energy Sciences, Office of Science, US Department of Energy.

References

[1] L.J. Kieffer, G.H. Dunn, Rev. Mod. Phys. 38 (1966) 1, and references therein.
[2] T.D. Märk, G.H. Dunn (Eds.), Electron Impact Ionization, Springer, Wien, 1985.
[3] R.S. Freund, in Swarm Studies and Inelastic Electron Molecule Collisions, L.C. Pitchford, B.V. McKoy, A. Chutjian, S. Trajmar (Eds.), Springer, New York, 1987, p. 329.
[4] T.D. Märk, in Linking the Gaseous and Condensed Phases of Matter, L.G. Christophorou, E. Illenberger, W.F. Schmidt (Eds.), Plenum, New York, NATO ASI Series 326, 1994, p. 155.
[5] K. Becker (Ed.), Novel Aspects of Electron-Molecule Collisions, World Scientific, Singapore, 1998.
[6] R. Basner, K. Becker, H. Deutsch, M. Schmidt, in M. Inokuti, K. Becker (Eds.), Advances in Atomic, Molecular, and Optical Physics, Vol. 43, Academic, New York, 1999, pp. 147–185.
[7] M.R.H. Rudge, Rev. Mod. Phys. 40 (1968) 564.
[8] S.M. Younger, in T.D. Märk, G.H. Dunn (Eds.), Electron Impact Ionization, Springer Verlag, Vienna, 1985.
[9] S.M. Younger, T.D. Märk, in T.D. Märk, G.H. Dunn (Eds.), Electron Impact Ionization, Springer Verlag, Vienna, 1985.
[10] R.K. Janev (Ed.), Atomic and Molecular Processes in Fusion Edge Plasmas, Plenum, New York, 1995.
[11] V. Tarnovsky, K. Becker, Plasma Sources Sci. Technol. 4 (1995) 307.
[12] J.W. Ötvos, D.P. Stevenson, J. Am. Chem. Soc. 78 (1956) 546.
[13] W.L. Fitch, A.D. Sauter, Anal. Chem. 55 (1983) 832.
[14] H. Deutsch, M. Schmidt, Beitr. Plasmaphys. 24 (1984) 475, and references therein to earlier publications.
[15] H. Deutsch, K. Becker, T.D. Märk, Int. J. Mass Spectrom. Ion Processes 167/168 (1997) 503.
[16] H. Deutsch, K. Becker, R. Basner, M. Schmidt, T.D. Märk, J. Phys. Chem. 106 (1998) 8819.
[17] M. Bobeldijk, W.J. van der Zande, P.G. Kistemaker, Chem. Phys. 179 (1994) 125.
[18] C.G. Aitken, D.A. Blunt, P.W. Harland, J. Chem. Phys. 101 (1994) 11 074.
[19] C.G. Aitken, D.A. Blunt, P.W. Harland, Int. J. Mass Spectrom. Ion Processes 149/150 (1995) 279.
[20] C. Vallance, P.W. Harland, R.G.A.R. Maclagan, J. Phys. Chem. 100 (1996) 15 021.
[21] D. Margreiter, H. Deutsch, M. Schmidt, T.D. Märk, Int. J. Mass Spectrom. Ion Processes 100 (1990) 157.
[22] H. Deutsch, C. Cornelissen, L. Cespiva, V. Bonacic-Koutecky, D. Margreiter, T.D. Märk, Int. J. Mass Spectrom. Ion Processes 129 (1993) 43.
[23] H. Deutsch, T.D. Märk, V. Tarnovsky, K. Becker, C. Cornelissen, L. Cespiva, V. Bonacic-Koutecky, Int. J. Mass Spectrom. Ion Processes 137 (1994) 77.
[24] D.K. Jain, S.P. Khare, J. Phys. B 9 (1976) 1429.
[25] S.P. Khare, W.J. Meath, J. Phys. B 20 (1987) 2101.
[26] Y.-K. Kim, M.E. Rudd, Phys. Rev. A 50 (1994) 3954.
[27] W. Hwang, Y.-K. Kim, M.E. Rudd, J. Chem. Phys. 104 (1996) 2956.
[28] Y.-K. Kim, W. Hwang, N.M. Weinberger, M.A. Ali, M.E. Rudd, J. Chem. Phys. 106 (1997) 1026.
[29] We note in this context that both the DM formalism and

the BEB formalism calculate the counting ionization cross section for a molecule (for a definition see [2]), i.e. the sum of all partial ionization cross sections involving the removal of a single electron from the parent molecule. In the case of most molecules the counting ionization cross section is equal to the total ionization cross section because cross sections for multiple ionization are generally rather small (see [2]).

[30] N.F. Mott, Proc. R. Soc. London Ser. A 126 (1930) 259.
[31] L.D. Landau, E.M. Lifshitz, Quantum Mechanics—Non-relativistic Theory, Addison-Wesley, Reading, MA, p. 575.
[32] M. Inokuti, Rev. Mod. Phys. 43 (1971) 297.
[33] H. Bethe, Ann. Phys. 5 (1930) 325.
[34] J.H. Miller, W.E. Wilson, S.T. Manson, M.E. Rudd, J. Chem. Phys. 86 (1987) 157.
[35] D.K. Jain, S.P. Khare, Indian J. Pure Appl. Phys. 14 (1976) 201.
[36] S.P. Khare, B.D. Padalia, R.M. Nayak, Can. J. Phys. 52 (1974) 1755.
[37] A.E.S. Green, T. Sawada, J. Atmos. Terr. Phys. 70 (1972) 1719.
[38] S.P. Khare, Planet. Space Sci. 17 (1969) 1257.
[39] R. Shingal, B.B. Srivastava, S.P. Khare, J. Chem. Phys. 61 (1974) 4656.
[40] S.P. Khare, S. Prakash, W.J. Meath, Int. J. Mass Spectrom. Ion Processes 88 (1989) 299.
[41] S. Pal, S. Prakash, S. Kumar, Int. J. Mass Spectrom. Ion Processes 164 (1997) 14.
[42] S. Pal, S. Prakash, S. Kumar, Int. J. Mass Spectrom. Ion Processes 174 (1998) 247.
[43] S. Pal, S. Prakash, Rapid Commun. Mass Spectrom. 12 (1998) 297.
[44] S. Pal, S. Prakash, S. Kumar, Int. J. Mass Spectrom. Ion Processes 184 (1999) 201.
[45] W.F. Miller, R.L. Platzmann, Proc. Phys. Soc. A 70 (157) 299.
[46] C.B. Opal, E.C. Beaty, W.K. Peterson, At. Data 4 (1972) 209.
[47] N. Djuric, D. Belic, M. Kurepa, J.U. Mack, J. Rothleitner, T.D. Märk, Proceedings of the 12th International Conference on the Physics of Electronic and Atomic Collisions, Gatlinburg, North Holland, Amsterdam, 1985, S. Datz (Ed.), p. 384.
[48] F.F. Rieke, W. Prepejchal, Phys. Rev. A 6 (1972) 1507.
[49] V. Saksena, M.S. Kushwaha, S.P. Khare, Physica B 233 (1997) 201, and Int. J. Mass Spectrom. Ion Processes 171 (1997) L1.
[50] R. Mayol, F. Salvat, J. Phys. B 23 (1990) 2117.
[51] S.P. Khare, M.K. Sharma, S. Tormar, J. Phys. B 32 (1999) 3147.
[52] L. Vriens, in Case Studies in Atomic Physics, Vol. 1, E.W. McDaniel, M.R.C. McDowell (Eds.), North Holland, Amsterdam, 1969, p. 335.
[53] M.E. Rudd, Y.K. Kim, D.H. Madison, T.J. Gay, Rev. Mod. Phys. 64 (1992) 441.
[54] M.A. Ali, Y.K. Kim, W. Hwang, N.M. Weinberger, M.E. Rudd, J. Chem. Phys. 106 (1997) 9602.
[55] H. Nishimura, W.M. Huo, M.A. Ali, Y.K. Kim, J. Chem. Phys. 110 (1999) 3811.
[56] J. Berkowitz, Photoabsorption, Photoionization, and Photoelectron Spectroscopy, Academic, New York, 1979.
[57] J.W. Gallagher, C.E. Brion, J.A.R. Samson, F.W. Langhoff, J. Phys. Chem. Ref. Data 17 (1988) 9, and references therein.
[58] H. Deutsch, T.D. Märk, Int. J. Mass Spectrom. Ion Processes 79 (1987) R1.
[59] D. Margreiter, H. Deutsch, T.D. Märk, Int. J. Mass Spectrom. Ion Processes 139 (1994) 127.
[60] D. Margreiter, H. Deutsch, T.D. Märk, Contrib. Plasma Phys. 30 (1990) 487.
[61] H. Deutsch, K. Becker, S. Matt, T.D. Märk, J. Phys. B 32(1999) 4249.
[62] H. Deutsch, T.D. Märk, Contrib. Plasma Phys. 34 (1994) 19.
[63] H. Deutsch, D. Margreiter, T.D. Märk, Z. Phys. D 29 (1994) 31.
[64] H. Deutsch, K. Becker, J. Pittner, V. Bonacic-Koutecky, S. Matt, T.D. Märk, J. Phys. B 29 (1996) 5175.
[65] H. Deutsch, K. Becker, T.D. Märk, Int. J. Mass Spectrom. Ion Processes 144 (1995) L9.
[66] H. Deutsch, K. Becker, S. Matt, T.D. Märk, J. Chem. Phys. 111 (1999) 1964.
[67] H. Deutsch, T.D. Märk, Nucl. Instrum. Meth. Phys. Res. B 98 (1995) 135.
[68] H. Deutsch, K. Becker, T.D. Märk, Int. J. Mass Spectrom. Ion Processes 151 (1995) 207.
[69] H. Deutsch, K. Becker, T.D. Märk, Contrib. Plasma Phys. 35 (1995) 421.
[70] H. Deutsch, K. Becker, T.D. Märk, J. Phys. B 29 (1996) L497.
[71] H. Deutsch, K. Becker, D.P. Almeida, T.D. Märk, Int. J. Mass Spectrom. Ion Processes 171 (1997) 115.
[72] H. Deutsch, K. Becker, S. Matt, T.D. Märk, Plasma Phys. Controlled Fusion 40 (1998) 1721.
[73] J.J. Thomson, Philos. Mag. 23 (1912) 449.
[74] M. Gryzinski, Phys. Rev. A 138 (1965) 305.
[75] D. Margreiter, Ph.D. Thesis 1992, Universität Innsbruck, unpublished.
[76] M.S. Mott, H.S.W. Massey, The Theory of Atomic Collisions, Oxford University Press, Oxford, UK, 1943, p. 243.
[77] J.S. Mann, J. Chem. Phys. 46 (1967) 1646.
[78] P. Tiwari, D.K. Rai, M.L. Rustgi, J. Chem. Phys. 73 (1980) 3040.
[79] H. Deutsch, K. Becker, T.D. Märk, Int. J. Mass Spectrom. Ion Processes 177 (1998) 47.
[80] H. Deutsch, K. Becker, T.D. Märk, Int. J. Mass Spectrom. Ion Processes 185/186/187 (1999) 319.
[81] R.S. Mulliken, J. Chim. Phys. 46 (1949) 675.
[82] R. Tang, J. Callaway, J. Chem. Phys. 84 (1986) 6858.
[83] S.V. Khristenko, A.I. Maslov, V.P. Shevelko, Molecules and Their Spectroscopic Properties, Springer Series on Atoms and Plasmas, Springer Verlag, New York, 1998.
[84] High Performance Computational Chemistry Group, NWChem, A Computational Chemistry Package for Parallel

Computers, Version 3.2, 1998, Pacific Northwest National Laboratory, Richland, WA 99352.
[85] M. Terrissol, M.C. Bordage, V. Caudrekier, P. Segur, Cross Sections for 0.025–1 keV Electrons and 10 eV–1 keV Photons, in Atomic and Molecular Data for Radiotherapy, IAEA-TECDOC-506, International Atomic Energy Agency, Vienna, 1989.
[86] J.P. Desclaux, At. Data Nucl. Data Tables 12 (1973) 325.
[87] S.G. Lias, J.E. Bartmess, J.F. Liebman, J.L. Holmes, R.D. Levin, W.G. Mallard, J. Phys. Chem. Ref. Data 17 (1988) 621 (suppl.).
[88] O.J. Orient, S.K. Srivastava, J. Phys. B 20 (1987) 3923.
[89] H.C. Straub, D. Lin, B.G. Lindsay, K.A. Smith, R.F. Stebbings, J. Chem. Phys. 106 (1997) 4430.
[90] N. Djuric, I. Cadez, M. Kurepa, Int. J. Mass Spectrom. Ion Processes 108 (1991) R1.
[91] D. Rapp, P. Englander-Golden, J. Chem. Phys. 43 (1965) 1465.
[92] B. Adamczyk, A.J.H. Boerboom, B.L. Schram, J. Kistemaker, J. Chem. Phys. 44 (1966) 4640.
[93] H. Nishimura, H. Tawara, J. Phys. B 27 (1994) 2063.
[94] V. Tarnovsky, K. Becker, in The Physics of Electronic and Atomic Collisions, Invited Papers of the XVIII International Conference on the Physics of Electronic and Atomic Collisions (ICPEAC), Aarhus, Denmark, 1993, T. Andersen, B. Fastrup, F. Fokmann, H. Knudsen, N. Andersen (Eds.), AIP Conference Proceedings, Vol. 295, AIP, New York, 1994, p. 234.
[95] F.A. Baiocchi, R.C. Wetzel, R.S. Freund, Phys. Rev. Lett. 53 (1984) 771.
[96] V. Tarnovsky, A. Levin, H. Deutsch, K. Becker, J. Phys. B 29 (1996) 139.
[97] V. Tarnovsky, H. Deutsch, K. Becker, J. Chem. Phys. 105 (1996) 6315.
[98] T.D. Märk, F. Egger, J. Chem. Phys. 67 (1977) 2629.
[99] T.D. Märk, F. Egger, M. Cheret, J. Chem. Phys. 67 (1977) 3795.
[100] R. Basner, M. Schmidt, H. Deutsch, V. Tarnovsky, A. Levin, K. Becker, J. Chem. Phys. 103 (1995) 77.
[101] B.L. Schram, M.J. van der Wiel, F.J. de Heer, H.R. Moustafa, J. Chem. Phys. 44 (1966) 49.
[102] H. Chatham, D. Hils, R. Robertson, A.C. Gallagher, J. Chem. Phys. 81 (1984) 1770.
[103] V. Grill, G. Walder, P. Scheier, M. Kurdel, T.D. Märk, Int. J. Mass Spectrom. Ion Processes 129 (1993) 31.
[104] S.-H. Zheng, S.K. Srivastava, J. Phys. B 29 (1996) 3235.
[105] J.T. Tate, P.T. Smith, Phys. Rev. 39 (1932) 270.
[106] A. Gaudin, R. Hagemann, J. Chem. Phys. 64 (1967) 1209.
[107] F.W. Lampe, J.L. Franklin, F.H. Field, J. Am. Chem. Soc. 79 (1957) 6129.
[108] H.U. Poll, C. Winkler, D. Margreiter, V. Grill, T.D. Märk, Int. J. Mass Spectrom. Ion Processes 112 (1992) 1.
[109] M.R. Bruce, R.A. Bonham, Int. J. Mass Spectrom. Ion Processes 123 (1993) 97.
[110] M.V.V.S. Rao, S.K. Srivastava, Contributed Papers, XXth International Conference on the Physics of Electronic and Atomic Collisions (ICPEAC), Abstract Mo150, F. Aumayr, G. Betz, H.P. Winter (Eds.), July 1997, Vienna, Austria.
[111] J.A. Beran, L. Kevan, J. Phys. Chem. 73 (1969) 3866.
[112] V. Tarnovsky, K. Becker, J. Chem. Phys. 98 (1993) 7686.
[113] V. Tarnovsky, P. Kurunczi, D. Rogozhnikov, K. Becker, Int. J. Mass Spectrom. Ion Processes 128 (1993) 181.
[114] V. Tarnovsky, A. Levin, K. Becker, R. Basner, M. Schmidt, Int. J. Mass Spectrom. Ion Processes 133 (1994) 175.
[115] V. Tarnovsky, A. Levin, K. Becker, J. Chem. Phys. 100 (1994) 5626.
[116] T.R. Hayes, R.C. Wetzel, F.A. Baiocchi, R.S. Freund, J. Chem. Phys. 88 (1989) 823.
[117] T.R. Hayes, R.J. Shul, F.A. Baiocchi, R.C. Wetzel, R.S. Freund, J. Chem. Phys. 89 (1989) 4035.
[118] R.J. Shul, T.R. Hayes, R.C. Wetzel, F.A. Baiocchi, R.S. Freund, J. Chem. Phys. 89 (1989) 4042.
[119] H.U. Poll, J. Meichsner, Contrib. Plasma Phys. 27 (1987) 359.
[120] M.V. Kurepa, 3rd Cz. Conference on Electronics and Vacuum Transactions (1965) (as quoted in [124]).
[121] D. Margreiter, G. Walder, H. Deutsch, H.U. Poll, C. Winkler, K. Stephan, T.D. Märk, Int. J. Mass Spectrom. Ion Processes 100 (1990) 143.
[122] Y.B. Kim, M.E. Rudd, Comments At. Mol. Phys. 34 (1999) 309.
[123] B.L. Schram, F.J. de Heer, M.J. van der Wiel, J. Kistemaker, Physica 31 (1965) 94.
[124] B.L. Schram, H.R. Moustafa, J. Schutten, F.J. de Heer, Physics 32 (1966) 734.
[125] E. Krishnakumar, S.K. Srivastava, Int. J. Mass Spectrom. Ion Processes 113 (1992) 1.
[126] H.C. Straub, P. Renault, B.G. Lindsay, K.A. Smith, R.F. Stebbings, Phys. Rev. A 54 (1996) 2146.
[127] See calculated data given in [49].
[128] D.R. Schultz, L. Meng, R.E. Olson, J. Phys. B 25 (1992) 4601.
[129] R.S. Freund, R.C. Wetzel, R.J. Shul, Phys. Rev. A 41 (1990) 5861.
[130] See, e.g. M.W. Chase Jr., K.A. Davis, J.R. Downey, D.J. Frurip, R.A. McDonald, A.N. Syverud, J. Phys. Chem. Ref. Data 14 (1985) 1.
[131] M.W. Siegel, Int. J. Mass Spectrom. Ion Processes 44 (1982) 19.
[132] K.A. Newson, S.M. Lee, S.D. Price, N.J. Mason, Int. J. Mass Spectrom. Ion Processes 148 (1995) 203.
[133] N. Djuric, I.M. Cadez, M.V. Kurepa, Int. J. Mass Spectrom. Ion Processes 83 (1988) R7.
[134] M.A. Bolorizadeh, M.E. Rudd, Phys. Rev. A 33 (1986) 882.
[135] J. Schutten, F.J. de Heer, H.R. Mustafa, A.J.H. Boerbom, J. Kistemaker, J. Chem. Phys. 44 (1966) 3924.
[136] H.C. Straub, B.G. Lindsay, K.A. Smith, R.F. Stebbings, J. Chem. Phys. 108 (1998) 109.
[137] M.V.V.S. Rao, S.K. Srivastava, J. Phys. B 25 (1992) 2175.
[138] K. Bederski, L. Woitek, B. Adamczyk, Int. J. Mass Spectrom. Ion Processes 35 (1980) 171.
[139] A. Crowe, J.W. McConkey, Int. J. Mass Spectrom. Ion Processes 24 (1977) 181.

[140] H.C. Straub, B.G. Lindsay, K.A. Smith, R.F. Stebbings, J. Chem. Phys. 105 (1996) 4015.
[141] T.W. Shyn, W.E. Sharp, Phys. Rev. A 20 (1979) 2332.
[142] N. Djuric, I. Cadez, M. Kurepa, Fizika 21 (1989) 339.
[143] R. Basner, M. Schmidt, private communication (1999) and to be published.
[144] L.G. Christophorou, D.L. McCorkle, A.A. Christodoulides, in Electron-Molecule Collisions and Their Applications, Vol. 1, L.G. Christophorou (Ed.), Academic, New York, 1984, p. 478.
[145] M.R. Bruce, C. Ma, R.A. Bonham, Chem. Phys. Lett. 190 (1992) 285.
[146] Y.K. Kim, private communication (1999) and to be published.